Integrated Master in Chemical Engineering

Chromatographic Separation of Dyes in a Fixed Bed Adsorber

Master's Dissertation

by

Albertina Gonçalves Rios

Developed for the dissertation course unit

at

LSRE - Laboratory of Separation and Reaction Engineering

Supervisor: **Dr. Alexandre Ferreira**

Co-Supervisors: **Prof. José Miguel Loureiro**

Prof. Adélio Mendes

Chemical Engineering Department

July 2017

“Our knowledge can only be finite,
while our ignorance must necessarily be infinite”
Karl Popper

Acknowledgments

Deixo esta secção para agradecer a todos aqueles que direta ou indiretamente contribuíram para a realização deste trabalho.

Gostaria de agradecer aos meus orientadores Dr. Alexandre Ferreira, Prof. José Miguel Loureiro e Prof. Adélio Mendes pela oportunidade e encorajamento durante a realização deste trabalho. Um especial agradecimento ao orientador Dr. Alexandre Ferreira uma vez que sem todo o seu apoio e orientação, este trabalho não teria corrido da mesma forma.

Deixo também um agradecimento ao Eng. Luís Carlos Matos por toda a sua ajuda no laboratório ao longo destes meses.

Quero também agradecer ao Jonathan Gonçalves pela sua ajuda com o manuseamento da extrusora, que foi fundamental para a produção dos granulados.

Desejo agradecer à Dra. Mafalda Ribeiro por todo o seu apoio durante estes meses.

À amiga Joana Matos o meu muito obrigado por todo o apoio e companheirismo.

Às colegas Ana Chaves e Mayuri Pratapsi pelo trabalho que tinham já realizado, que permitiu validar alguns dos resultados obtidos.

Por último e não menos importante, queria agradecer aos meus amigos e família, em especial aos meus pais e ao meu irmão por todo o apoio.

Este trabalho foi financiado por: Projeto POCI-01-0145-FEDER-006984 - Laboratório Associado LSRE-LCM - financiado pelo Fundo Europeu de Desenvolvimento Regional (FEDER), através do COMPETE2020 – Programa Operacional Competitividade e Internacionalização (POCI) e por fundos nacionais através da Fundação para a Ciência e a Tecnologia I.P.

Abstract

Since environmental pollution affects more people day after day it is necessary to implement measures with the aim of preserving the nature. One important issue is related with the water pollution and one of the causes is dyed wastewater, coming from various industries. Therefore one of the most efficient ways to solve or minimize this problem is adsorption based processes which is the main topic of this document.

As the main goal of this manuscript is to propose an experimental experimental protocol for the curricular unit of *Práticas de Engenharia Química III,* it was necessary to test adsorbents with different dyes in order to obtain the fundamental necessary know-how. Adsorption equilibrium isotherms were determined with MCM-41 adsorbent for different. After choosing the adsorbent it was necessary to shape its powder with the aim of using it in column and batch experiments.

Kinetic tests were performed with this adsorbent and with other two, SBA-15 and a carbon based xerogel. These essays were useful to assess the adsorption process kinetics, that is, to understand the existence of kinetics limitations.

Another important goal was finding an efficient method of regeneration of the adsorbent, which turn out to be possible in an efficient way with a mixture of acetone, water and hydrochloric acid.

Breakthrough experiments were performed with two dyes, BB41 (Basic Blue 41) and BR18 (Basic Red 18) and adsorption capacities of 189 $mg \cdot g^{-1}$ and $14 \cdot mg \cdot g^{-1}$ were obtained, respectively. Once the breakthrough experiments take a long time, being impossible to adapt the experimental work to a three hours lab class, pulse experiments were proposed instead with a mixture of two differently charged dyes with the objective of separating them in a packed column. This goal was achieved with the mixture of dyes: Basic Blue 41, which is a cationic dye, so it was retained in the adsorbent and the dye Orange II (O II) which is anionic so it was not retained in the adsorbent.

Keywords (theme): adsorption, chromatographic separation, dyes, MCM-41.

Resumo

Uma vez que o ambiente preocupa cada vez mais pessoas, dia após dia, é necessário a implementação de medidas com o objetivo de preservar a natureza. Uma questão importante encontra-se relacionada com a poluição da hidrosfera, sendo uma das possíveis causas relacionada com os efluentes corados, provenientes das mais variadas industrias. Assim sendo, uma das técnicas mais eficientes desenvolvidas com o intuito de resolver ou minimizar este problema é a adsorção, sendo que este é o principal tópico deste manuscrito.

Com o objetivo de obter uma proposta de trabalho experimental e respetivo protocolo experimental para a unidade curricular Práticas de Engenharia Química III foi estudada a adsorção de diferentes corantes em vários adsorventes, de modo a perceber qual seria a combinação mais eficaz. Assim, foram determinadas isotérmicas de equilíbrio de adsorção com o adsorvente MCM-41 para diferentes corantes. Após a escolha do adsorvente foi necessário a obtenção de granulados a partir do adsorvente em pó, de modo a ser possível a sua utilização nos vários testes.

Foram também efetuados testes cinéticos com este adsorvente referido, bem como com outros dois, SBA-15 e carvão ativado xerogel. Estes testes permitiram perceber a possível existência de limitações cinéticas.

Outro objetivo importante era encontrar um método eficiente de regeneração do adsorvente, tendo sido concretizado através da utilização de uma mistura de acetona, água e ácido clorídrico.

Foram também obtidas curvas de rutura com dois corantes, BB41 (Azul Básico 41) e BR18 (Vermelho Básico 18), tendo sido obtidas capacidades de adsorção de 189 $mg \cdot g^{-1}$ e 14 $mg \cdot g^{-1}$, respetivamente.

Uma vez que os ensaios para a determinação de curvas de rutura eram bastante demorados, sendo impossível a sua implementação para uma aplicação como protocolo experimental no tempo útil de uma aula laboratorial, foram também realizados testes com uma entrada em pulso, utilizando dois corantes de diferente carga, sendo objetivo a sua separação em coluna. Foi possível concretizar este objetivo, na medida em que foi utilizada uma mistura de corantes, o corante Azul Básico 41, o qual é catiónico, e portanto é adsorvido e o corante Laranja II (O II), o qual é aniónico e por essa mesma razão não e adsorvido pelo adsorvente selecionado.

Palavras-chave: Adsorção, separação cromatográfica, corantes, MCM-41.

Declaration

Declaro, sob compromisso de honra, que este trabalho é original e que todas as contribuições não originais foram devidamente referenciadas com identificação da fonte.

Porto, 3 de julho de 2017

Albertina Gonçalves Rios

(Albertina Gonçalves Rios)

Index

Notation and Glossary

A	Area	m^2
c	Concentration in the liquid phase	$mol \cdot l^{-1}$
C_∞	Equilibrium Concentration	$mol \cdot l^{-1}$
C_0	Feed Concentration	$mol \cdot l^{-1}$
K_F	Freundlich constant	$mol \cdot kg^{-1} \cdot (l \cdot mol^{-1})^{1/n}$
K_L	Constant related to the free energy of adorption	$l \cdot mol^{-1}$
l	length of the light path	cm
m_{ads}	Adsorbent amount	kg
n	Inverse of the adsorption intensity	
Q	Flowrate	$l \cdot min^{-1}$
Q_m	Maximum adsorption quantity	$mol \cdot kg^{-1}$
q	Concentration in the solid	$mol \cdot kg^{-1}$
t	Time	min
t_{BP}	Breakthrough time	h
t_{st}	Stoichiometric time	h
u_0	Superficial fluid velocity	$cm \cdot s^{-1}$
u_i	Interstitial fluid velocity	$cm \cdot s^{-1}$
V_e	Eluted Volume	ml
z	Axial position	m

Greek leters

ε	Porosity	
λ	Wavelength	nm
ϕ	Solute flux	

List of Acronyms

BB41	Basic Blue 41
BR18	Basic Red 18
EDS	Dispersive X-Ray Spectroscopy
MB	Methylene Blue
MCM-41	Mobil composition of matter 41
O II	Orange II
RR239	Reactive Red 239
SBA-15	Santa Barbara acids
SEM	Scanning electron microscopy
XRD	X-Ray Diffraction

1 Introduction

1.1 Framing and presentation of the work

Once the environment pollution is increasing and it is necessary to take care and preserve the planet it is essential to implement preventive actions.

Dyes are used in many kinds of industries such as textile, paper, food, cosmetics and plastics. The effluents produced when these compounds are used need treatment before their discharge into hydrosphere. If they are not treated they will be a source of water pollution once they will give an undesirable color to water which reduces the sunlight penetration, representing a risk for aquatic life. Furthermore, some of them are toxic [1].

There many techniques used to treat dyeing wastewater, but the most used is the adsorption technique. This separation method is an efficient process, which is characterized by the presence of two phases, the solute, also known as adsorbate and the adsorbent, which is a solid. The fluid adheres into the solid surface due to the existence of attractive forces, making possible the separation of the solid, the solute, from the solution.

In this work, as the main objective obtaining an experimental activity for the curricular unit of *Práticas de Engenharia Química III*, the adsorption of different dyes into different adsorbents is studied with the aim of finding the best combination of dye / adsorbent. The fundamental adsorption properties such as adsorption equilibrium as well as adsorption kinetics were assessed.

The integration of the knowledge obtained during this work led to a proposal of an experimental work, and respective experimental protocol – on the chromatographic separation of two dyes in a fixed bed column.

1.2 Outline

This work is divided in main seven chapters, the introduction, the context and state of the art, material and methods, the results and discussion, the experimental protocol for the laboratory experiment, the conclusions and the assessments of the work done.

The state of the art contains the information related to dyes, adsorbents, fixed bed adsorption, dyeing wastewater treatments.

The Chapter 3, material and methods contains the information related to the dyes analysis method, spectrophotometry, the adsorbent preparation and characterization. It also contains

the dyes selection and the regeneration procedure of the adsorbent. Finally it has a brief description of the experimental protocols for assessing the adsorption equilibrium data and adsorption kinetics, as well as the experimental protocol for the fixed bed experiments, breakthrough and pulse experiments.

Chapter 4, Results and Discussion, covers the adsorption equilibrium isotherms, kinetics and fix bed results and its discussion.

In Chapter 5 is elaborated an experimental protocol of the chromatographic separation of two dyes, in a fixed-bed column. This experimental protocol will be proposed as possible work for the curricular unit of *Práticas de Engenharia Química III*, as integration of the theoretical contents of the curricular unit of *Processos Separação II*.

The Conclusion chapter summarizes the main conclusions of the experimental results.

Finally, the Assessments of the work done which contains the information about the achieved objectives and future work, and it is presented in Chapter 7 of this Manuscript.

2 Context and State of the art

2.1 Dyes

Dyes are usually colored compounds due to four reasons: first, they absorb light in the visible spectrum. Second, they have at least one chromophore, which is the component responsible for the color. Third, they have a conjugated system, which provides a structure with alternating double and single bonds. Finally, they exhibit resonance of electrons, what makes possible stabilization in organic compounds.

Beside the chromophores, dyes also have another group, known as auxochromes. Some examples are carboxylic acid, sulfonic acid, amino and hydroxyl groups. These groups are responsible for shift the color and they are frequently used to influence the dye solubility [2].

2.1.1 Dyes classification

Dyes can be classified according to their applications or by their chemical structure. The chemical structure groups dyes by their properties, which represents an advantage, but the most common way of classifying dyes is by their usage, which is more practical [3]. Therefore, regarding their potential application, dyes can be classified as:

Direct dyes: These compounds are water-soluble anionic dyes and when they are used in aqueous solution in the presence of electrolytes, it makes them substantive (with high affinity) to cellulosic fibers. So these type of dyes are mainly used to dye materials made from cellulose, such as cotton, jute, viscose or paper, without needing mordants (substance that is combined with the dye to helping fix it) as auxiliaries. They are easy to apply and have moderate price. Although their wet-fastness are only moderate. Despite, some treatments can be used to improve the fastness to washing [4].

Vat dyes: These compounds are mainly applied to cellulosic fibers. They are water-insoluble and contain at least two carbonyl groups (C=O), what permits to transform them into water-soluble ‘leuco compounds’[5]. They are converted in alkaline bath by the use of reducing agents, such as sodium dithionite in the presence of sodium hydroxide.[6] The sodium salts of the compound penetrate into the cellulose fibers. Then the dye is reoxidized and the insoluble compound is attached firmly to the fiber. These type of dyes are used when very high light and wet-fastness properties are needed. Although, they have a high price and they are difficult to apply [3].

Sulphur Dyes: They are used for dyeing cellulosic fibers. They are very complex in terms of structure and this is a small group of dyes. These type of dyes can be divided into three groups:[3]

- C.I. Sulphur dyes: this group consists of amorphous powders, insoluble in water, which can become solubilize by heating with water and sodium sulfide.
- C.I. Leuco Sulphur Dyes: these liquid dyes are presented in a reduced form and also contain additional reducing agents for stabilization.
- C.I. Solubilised Sulphur Dyes: These compounds are thiosulfate derivatives of Sulphur dyes. They are also known as Bunte salts. These dyes are prepared through the reaction between water-insoluble sulfur dyes and sulfite and bisulfite in the presence of atmospheric oxygen.

Sulphur dyes constitute an important class of dyes because they are low cost and they have good wet- fastness properties [5].

Azoic Dyes: They are water-insoluble azo compounds. These dyes are mainly used for dying cellulosic fibers, providing a wide range of bright hues. They are produced *in situ* in textile fibers by the interaction between a diazo and a coupling components [5].

Reactive dyes: An important characteristic of these dyes is that they form covalent bonds with the substrate (a fiber, usually cotton), which is colored during the application process. The dye molecule contains functional groups that can suffer addiction or substitution reactions with other groups present in textile fibers, such as OH, SH and NH_2. So these type of dyes have excellent color fastness and they are known for their brightness [3].

Disperse dyes: These dyes are significantly water-insoluble and nonionic. They are mostly used on polyester but they can also be used on nylon, cellulose, cellulose acetate and acrylic fibers. They have poor wet-fastness properties on these substrates. Disperse dyes can be used in thermal transfer printing. These dyes category are classified by sublimation temperature: Class A have the lowest sublimation temperature while Class D have the highest [5, 6].

Acid dyes: These type of dyes are water-soluble, anionic azo dyes. They can be applied to nylon, wool, silk and modified acrylics [3].

Basic dyes: They are water-soluble cationic compounds, applied to paper, polyacrylonitrile, modified nylons and modified polyesters. They produce colored cations in solution. Consequently, they are usually called cationic dyes. These dyes have high substantivity for the substrate [3].

Solvent dyes: These compounds are water insoluble, but they are soluble in other types of solvents. They do not have solubilizing groups such as sulfonic acid, carboxylic acid or quaternary ammonium. They can be used for coloring plastics, gasoline, oils and waxes [3].

In *Figure 1* is presented a diagram of the dye classes according to their type: anionic, cationic and nonionic.

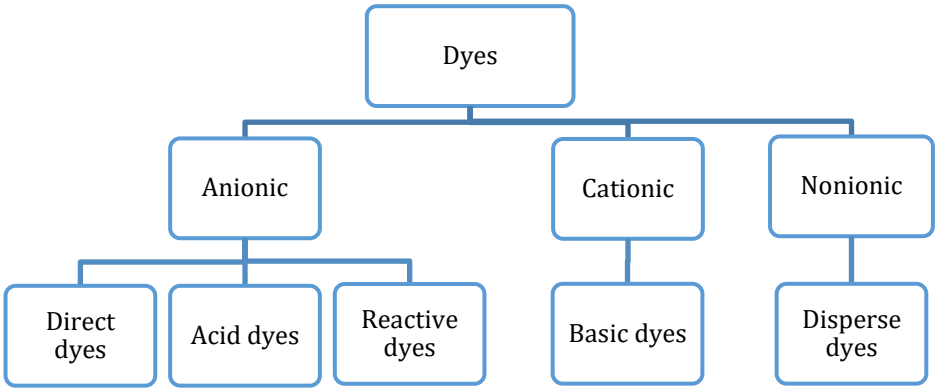

Figure 1 - Dyes classification

2.2 Dyeing wastewater treatments

There are many techniques developed to treat dyeing wastewater, which can be biological, chemical or physical [7]. Biological techniques can be divided into aerobic and anaerobic processes. The aerobic treatment can be used to purify water with the help of aerobic bacteria in an aerobic environment. On the other hand, anaerobic bacteria decomposes matter in the absence of air [8]. Some examples of chemical techniques are coagulation, electrolysis and oxidation methods. Coagulation occurs when, in a colloidal suspension, is added a coagulant, which is an electrolyte product, such as aluminum sulphate, ferric sulphate, ferric chloride and others. These compounds can eliminate the surface electrical charge. Another chemical treatment is chemical oxidation, whereby the dye is oxidized, bleaching the effluent. Fenton reaction (which is a process that uses hydrogen peroxide as oxidizing agent in an acidic solution containing Fe^{2+} ions) and ozone oxidation are two different processes of chemical oxidation [9,8]. Physical techniques include methods such as membrane separation and adsorption. For dyes removal through membrane separation, a pressure difference between the both sides of the membrane is needed. The major disadvantage of this kind of technology is that the membrane have limited lifetime and their replacement can be expensive [10]. These membrane processes can be nanofiltration, ultrafiltration, microfiltration and reverse osmosis [9]. Adsorption is the most used method in wastewater treatment. In this method, pollutants present in the wastewater, such as dyes, are adsorbed on the surface of the porous material, which permits its removal [8].

2.3 Adsorbents

The viability of an adsorption process depends on how the adsorbent performs regarding both fundamental properties, adsorption equilibrium and adsorption kinetics. Thus, a good adsorbent provides high adsorptive capacity and fast kinetics. To satisfy these requirements the solid should have high surface area or micropore volume, and have high pore network connectivity to transport molecules to the interior [11].

Pore sizes are classified in three ranges: macropores, which have diameters larger than 50 nm, mesopores, which have diameters in a range of 2-50 nm and micropores, which have diameters smaller than 2 nm. Included in micropores there are supermicropores, with a diameter range of 0.7-2 nm, ultramicropores with a diameter smaller than 0.7 nm and finally the submicropores with a diameter smaller than 0.4 nm [12,13].

The most common adsorbents are:

Alumina: This adsorbent is usually used in the removal of water from a gas stream. It has a high group functional density on the surface, which makes it suitable for polar compounds, such as water. It has a high surface area and high macropore volume [11].

Mesoporous silica: These are inorganic materials synthetized in the presence of surfactants. The production conditions influence the characteristics of porous structure and the macroscopic morphology. These materials have highly organized porosity, high surface area and high pore volume [14].

Silica gel: It is produced by reacting sodium silicate with acid [15]. This adsorbent is usually used for water removal because of its strong hydrophilicity. Depending on the preparation the surface area is in a range of 200 $m^2 \cdot g^{-1}$ to 900 $m^2 \cdot g^{-1}$ [11].

Activated carbons: This is a versatile adsorbent family because of its high surface area and micropore volume. The nature of the surface of these adsorbents is complex and it depends on factors such as the source of carbon or the way how the carbon is activated [11].

Zeolites: These type of adsorbents can be found naturally or made synthetically. There are many types of synthetic zeolites, such as type A zeolites (LTA structure), type X and type Y (FAU structure), modernite (MOR) and ZSM-5 and silicalite-1 (MFI) [11].

MOFs: They are made by joining metal-containing units with organic linkers, using strong bonds to obtain open crystalline frameworks with permanent porosity. MOFs have high porosity and a lot of possible usages [16].

2.4 Fixed bed adsorption

The adsorption process of a given component can be performed in a fixed bed column experiment or in a batch experiment. Fixed bed column operation can present some advantages at low solution concentrations if equilibrium isotherm is steep, since it allows a better use of the adsorbent, leading to a lower amount of adsorbent needed [17].

For the mass balance to the fixed bed column, it is necessary to define a volume element between z and $z + dz$ and it is presented in Figure 2.

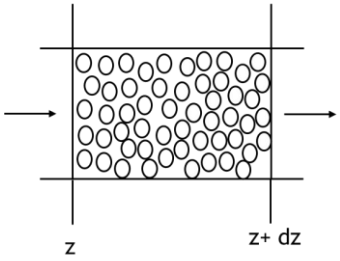

Figure 2 – Differential volume element.

The mass balance is represented by [18]:

$$A\emptyset_z = A\emptyset_{z+dz} + \varepsilon A\frac{dc}{dt}dz + (1-\varepsilon)A\frac{d < q >}{dt}dz \tag{2.1}$$

This mass balance is important to define the velocity of the concentrations wave within the column. Where, $\emptyset$ is the solute flux, ε is the bed porosity, c is the concentration of the solute in the fluid and $< q >$ is the average of adsorbate concentration in the solid.

Isothermal operation, negligible pressure drop, plug flow flux of the fluid phase, instantaneous adsorption equilibrium and negligible internal and external mass transfer resistances were considered [18]. Then through the calculation of the limit when $dz \to 0$ and considering only convective trasnsport, the flux becomes: $\emptyset = u_0 C$, being u_0 the superficial fluid velocity. It is also considered the relationship between the superficial fluid velocity and the interstitial velocity as $u_0 = u_i\varepsilon$, so it is obtained the equation 2. [18]

$$u_i\frac{\partial c}{\partial z} + \frac{\partial c}{\partial t} + \frac{(1-\varepsilon)}{\varepsilon}\frac{\partial < q >}{\partial t} = 0 \tag{2.2}$$

Assuming instantaneous equilibrium between the solid and liquid phases: $\langle q \rangle = q^* = f(c)$, that is, the average of concentrations in the solid is equal to the equilibrium solid concentration,(q^*) which is determined through the equilibrium adsorption isotherm ($f(c)$). It is obtained the equation 3, the partial derivate of the average concentration in the solid in order to time.

$$\frac{\partial < q >}{\partial t} = \frac{\partial q^*}{\partial t} = \frac{\partial f(c)}{\partial t} = \frac{df(c)}{dc}\frac{\partial c}{\partial t} = f'(c)\frac{\partial c}{\partial t} \tag{2.3}$$

Replacing in the equation 2, it is obtained the equation 4.

$$u_i \frac{\partial c}{\partial z} + \frac{\partial c}{\partial t} + \frac{(1-\varepsilon)}{\varepsilon} f'(c) \frac{\partial c}{\partial t} = 0 \tag{2.4}$$

The velocity of the concentration within the column is given by the equation 5 [18].

$$u_c = \left(\frac{dz}{dt}\right)_c = -\frac{\left(\frac{\partial c}{\partial t}\right)_z}{\left(\frac{\partial c}{\partial z}\right)_t} = \frac{u_i}{1 + \frac{(1-\varepsilon)}{\varepsilon} f'(c)} \tag{2.5}$$

This equation establishes that the concentration within the column is inversely proportional to the derivate of the isotherm.

In Figure 3 it is represented a scheme of a fixed bed column.

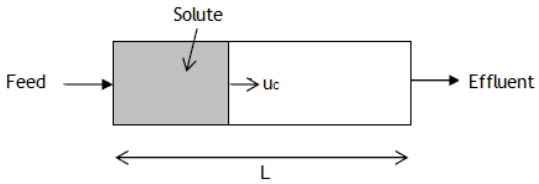

Figure 3 - Fixed bed column

Unfavorable isotherm

In Figure 4 is depicted an unfavorable isotherm.

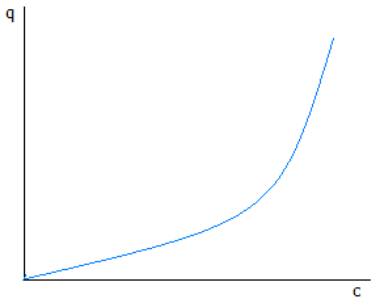

Figure 4 - Unfavorable isotherm

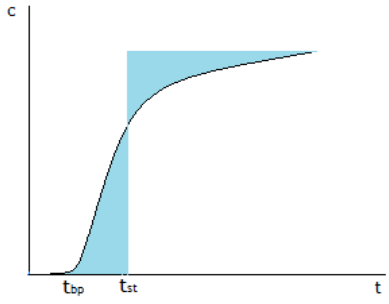

Figure 5 - Breakthrough curve

In this situation the $f'(c)$ increases with the increase of c and $f''(c) > 0$. Therefore, the lower concentrations travel faster than the larger concentrations, which originates a dispersive wave of concentrations. The breakthrough curve, which is the history of concentrations at the outlet of the column, has a dispersive nature as represented in Figure 5.

It is important to define the breakthrough time (t_{Bp}) which is the real operating time; it corresponds to the time at which the outlet concentration reaches a defined percentage (usually 1-5%) of the inlet concentration. Another important concept is the stoichiometric time

(t_{st}) which is the theoretical operating time; and it corresponds to the time needed to saturate the column if the wave were not dispersive and the front is equal to the feed. [18]

Favorable isotherm

In *Figure 6* is represented an example of a favorable isotherm.

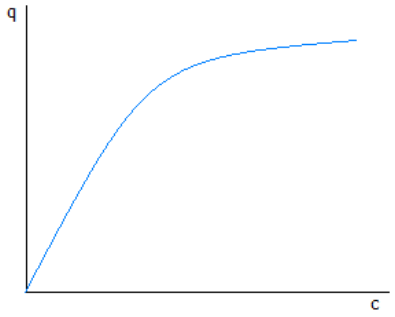

Figure 6 - Favorable isotherm

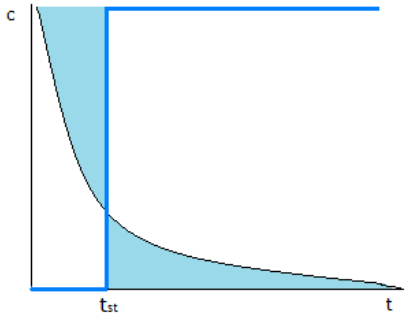

Figure 7 - Breakthrough curve

In this case the $f'(c)$ decreases with the increase of c and $f''(c) < 0$. Therefore, the larger concentrations travel faster than the lower concentrations. This originates a compressive wave of concentrations. In Figure 7 is represented, by the dark blue line, the breakthrough curve.

2.5 Dyes Adsorption

In the literature can be found several studies on the adsorption of natural and synthetic dyes in different adsorbents (e.g. activated carbons, mesoporous silicas, MOFs…); frequently used in the textile and food industry. Alazawi and co-workers studied adsorption of methylene blue (MB) in fixed-bed packed with SBA-15 [19]. They studied the dynamic capacity of the material as function of bed height, feed concentration, and feed flowrate. Therefore, the optimal conditions used were a bed height of 6 cm, an initial concentration of 40 $mg \cdot l^{-1}$ and a flow rate of 0.5 $ml \cdot min^{-1}$. Besides that the regeneration is possible, but it was noticed that the efficiency was reduced from 81 to 72% in 5 cycles and the percentage of removal was not changed significantly afterwards [19]. Karaca *et al*. also studied the adsorption of MB but using natural clays as adsorbent [20]. This study allowed the analysis of the influence of the initial dye concentration, temperature, and p_H. It was possible to conclude that de adsorbent capacity increases with the increasing of the initial dye concentration, as expected. On the other hand, it decreases with the increasing of temperature (also as expected) and p_H (except for the natural p_H of 5.6). Besides that, the authors reported that equilibrium was reached only after 1 hour [20]. Han *et al*. also studied the adsorption of MB and Rhodamine B (RhB) in batch with two different silica aerogels, hydrophobic silica aerogel (MSA) and hydrophilic silica aerogel (HAS) [21]. It was possible to conclude that RhB is better adsorbed by the HAS than MSA and

the adsorption of MB represents the opposite behavior, it is better adsorbed by the MSA than HAS. Besides that, it was tested the desorption efficiency, which is around 80% after the third cycle [21].

It is also possible to find, in the literature, studies with adsorbents from agricultural and industrial wastes.

Santos [22] studied the adsorption of textile dyes into inorganic matrix low-cost materials, such as industrial wastes and clays. The study focus on the performance of different dye/adsorbent systems: Basic Red 46/ Bentonitic clay, Basic Red 46/Sepiolite, Direct Blue 85/ Sepiolite, Reactive Blue 19/Waste Sludge, Acid Blue 193/Waste Sludge and Direct Blue 85/Waste Sludge. The effect of p_H, temperature, the presence of salts and other parameters were studied.

Idris and other co-works studied the adsorption of cationic and anionic dyes in agricultural solid wastes adsorbents, such as peanut hull, coir pith, rice husk and orange peel [23]. In this study it was possible to understand that the agricultural solid wastes are better for adsorbing the cationic dyes than anionic dyes. Besides that, it was noticed that p_H is the factor that most affects adsorption, being a high p_H value preferred for cationic dyes and a low p_H to the anionic dyes [23]. Sulak *et al*. also studied the adsorption in an adsorbent from agricultural waste. The authors used apricot stone activated carbon as adsorbent to remove a basic dye [24]. They studied the effect of the variation of the initial dye concentration, temperature, p_H and adsorbent dosage. It was noticed that the amount adsorbed increase with the increasing of the initial dye concentration, with the increasing of p_H and with the increasing of temperature [24].

It was found in the literature a few studies with mesoporous adsorbents. Sarkar *et al*. studied the performance of the adsorbent SBA-16 with the dyes Neutral Red (Basic Red 5, NR), Congo Red (CR), Safranin O (Basic Red 2, SF) and Reactive Red 2 (RR2) [25]. They also studied adsorption parameters such as p_H, contact time, temperature, dye concentration and adsorbent dosage. The authors analyzed the adsorbent and they reported that it has a high surface area, high average pore diameter, high total pore volume and high number of active sites. It was possible to conclude that the adsorption capacity of this adsorbent is more efficient for the removal of NR and SF dyes, which are cationic dyes than CR and RR2, which are anionic [25]. Mijowska *et al*. studied the efficiency adsorption of the anionic dye Direct Red 23 (DR23), nonionic dye Direct Green 97 (DG97) and the cationic dye Basic Yellow 23 (BY28) from aqueous solutions with a mesoporous carbon nanospheres (HMCN) adsorbent [26]. The equilibrium is well represented by the Langmuir isotherm. The authors also studied the influence of the initial dye concentration, temperature and p_H. It was possible to conclude that the adsorption capacity increases with the increasing of the initial dye concentration. For the p_H, the adsorptio depends on the charge of the dye. Therefore, for the DR23 and DG97, the adsorption capacity decreases with the increasing of p_H and the BY28 has the opposite behavior. The adsorption capacity

increases with the increasing of the temperature. From the results the authors obtained an adsorption capacity of 769.2 $mg \cdot g^{-1}$, 312.5 $mg \cdot g^{-1}$ and 909.1 $mg \cdot g^{-1}$ at 30 ºC for the DR23, DG97 and BY28, respectively [26].

Ang *et al*. resumed the factors that affect the adsorption of dyes [1]. One of the most important factors that affect adsorption is p_H. Adsorption of anionic dyes is favored when the surface is positively charged, being pH smaller than p_{Hpzc} (pH of zero charge). On the other hand, adsorption of cationic dyes is favored when p_H is higher than $p_{Hpzc,}$ i.e. with the surface negatively charged. The initial dye concentration is another important factor and with its increasing, the percentage of dye removal will decrease. On the other hand, the adsorption capacity increases with the increasing of the initial dye concentration, due to the higher mass transference with higher dye concentration. The authors also referred the effect of the temperature. Therefore, if the temperature increases during the adsorption, it represents an exothermic process, as in the physical adsorption. Finally mentioned the effect of the amount of adsorbent, being a large amount of adsorbent responsible for a higher dye removal percentage [1].

3 Material and Methods

3.1 Dyes selection

For the targeted studies were selected anionic and cationic dyes which properties are summarized in Table 1. These properties are the molecular formula, molecular weight and maximum wavelength. In Appendix 1 is presented the full table of dyes.

In Figure 8 are represented four possible combinations of binary mixtures with cationic and anionic dyes and one possible mixture with both cationic dyes, (Figure 11 d)). These combinations were made according to dye's molecular weight and the mixture color.

Table 1 - Dyes examples and its type, molecular formula, molecular weight and maximum wavelength.

Dye	Common name	Type	Molecular Formula	Molecular Weight ($g \cdot mol^{-1}$)	λ_{max} (nm)
Acid Orange 7	Orange II	Anionic	$C_{16}H_{11}N_2NaO_4S$	350.33	483
Basic Blue 9	Methylene Blue	Cationic	$C_{16}H_{18}ClN_3S$	319.85	664
Basic Blue 41	-	Cationic	$C_{20}H_{26}N_4O_6S_2$	482.57	590
Basic Red 18	-	Cationic	$C_{19}H_{25}Cl_2N_5O_2$	426.34	489
Reactive Red 239	-	Anionic	$C_{31}H_{19}ClN_7Na_5O_{19}S_6$	1136.32	542

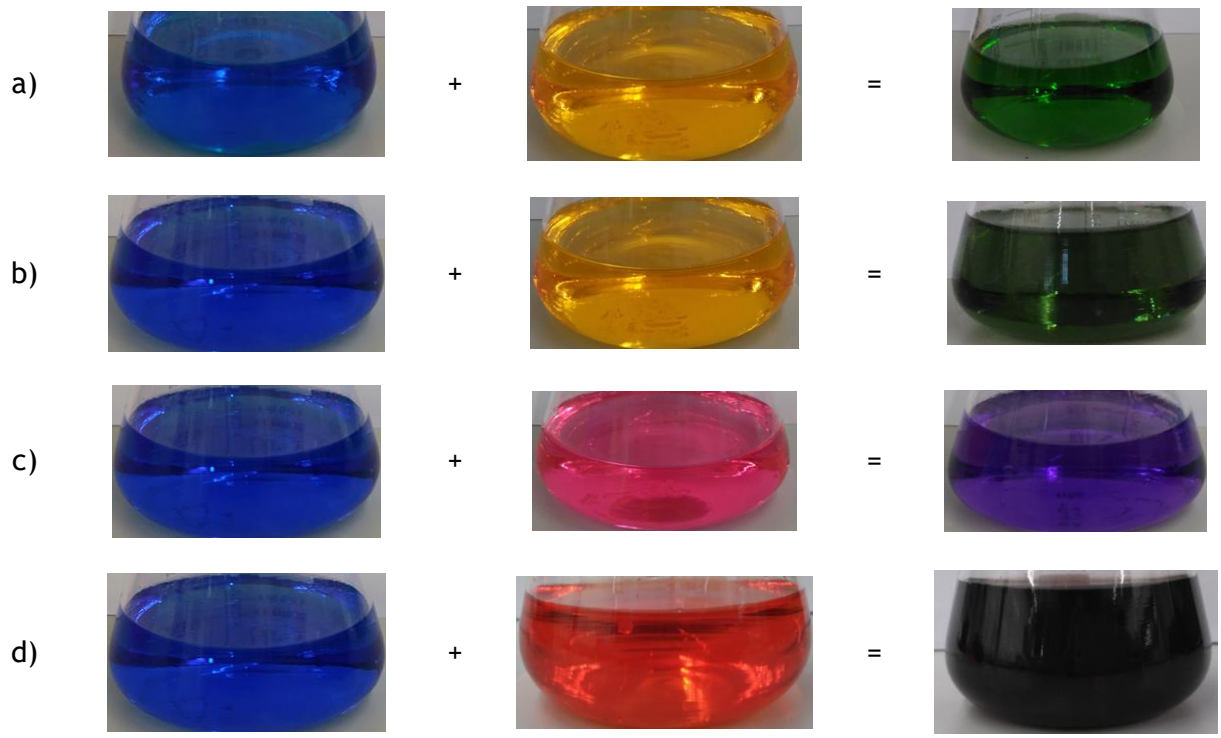

Figure 8 – Selected dyes and their binary mixtures a) Methylene Blue and Orange II; b) Basic Blue 41 and Orange II; c) Basic Blue 41 and Reactive Red 239; d) Basic Blue 41 and Basic Red 18.

3.2 Adsorbent selection

A mesoporous silica, MCM-41 was selected once the mesoporous adsorbents have high surface areas and high pore volume. Besides that, a mesoporous adsorbent could represent an advantage since it would not became an obstacle to the mass diffusion, as microporous structures are more prone to.

This adsorbent is also a good option for dyes separation since it only adsorbs cationic compounds due to its surface chemistry. The structure is characterized for having pore diameters between 35 and 40 Å and for being in a regular honeycomb arrangement such as the one represented in Figure 9.

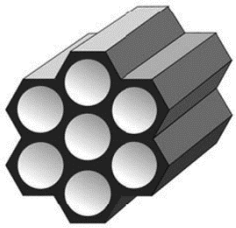

Figure 9 - MCM-41 honeycomb structure arrangement [36].

The MCM-41 powder (Figure 10) was purchased at ACS Material, USA.

Figure 10 – MCM-41 powder.

3.3 Adsorbent shaping and characterization

Once the experiment must be performed in a column it was necessary to obtain pellets from the powder adsorbent. A lab scale extruder was used in order to produce pellets (Caleva Multi Lab, UK). The extruder operating conditions were selected after several trials, and they are a velocity of mixture of 80 rpm and a velocity of extrusion of 45 rpm. The amount of water used was 5.7 ml per 5 g of powder. The obtained extrudates have 2 mm diameter. The pellets were submitted to calcination in order to increase their mechanical strength. Therefore, they were left in an oven for 12 h at a temperature of 120 ºC and then the temperature was risen to 550 ºC during 4 h.

After obtaining pellets, it was necessary to crush and sieve them, once it was noticed that the original extrudates only adsorb on the surface maybe due to mass transfer limitations (see Figure 11 a). Therefore the pellets were crushed and sieved to select the desired fraction, diameters between 0.25 mm and 0.60 mm. The obtained granulates are represented in Figure 11 b).

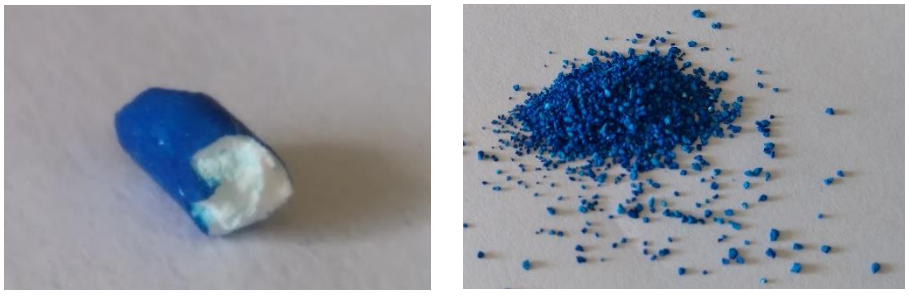

(a) (b)

Figure 11 – a) extrudates as obtained from the extruder after adsorption of Methylene Blue; b) granulates obtained after crushing and sieving.

MCM-41 granulates were characterized by a scanning electron microscopy (SEM) / Energy – Dispersive-X-Ray Spectroscopy (EDS) in Centro de Materiais da Universidade do Porto (CEMUP). In Figure 12 is presented the primitive particles observed through the SEM analyses inside the granulates. The particles exhibit an irregular form with a particle size between 200 nm and 900 nm. The EDS spectra obtained shows the presence of the elements Si, O and C, as it was expected once the composition of the material should be essentially Si and O since the molecular formula is SiO_2.

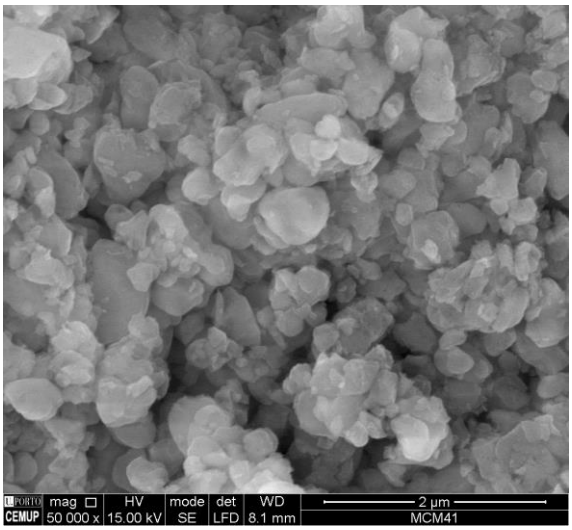

Figure 12 –Interior of a granulate.

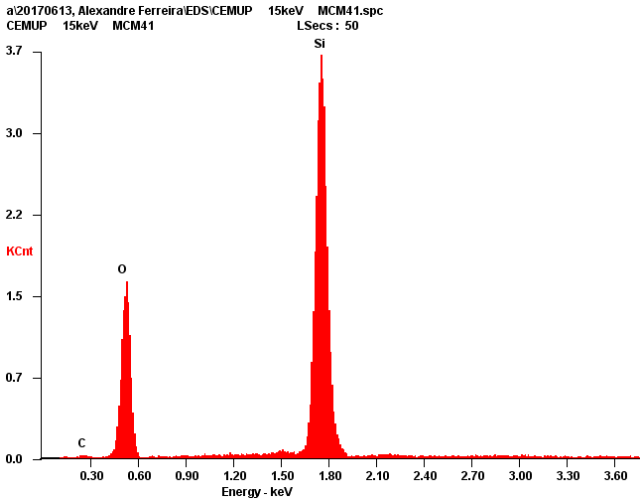

Figure 13 – EDS spectrum.

An X-Ray Diffraction (XRD) analysis was used to characterize the MCM-41 powder. This test was used to show the hexagonal symmetry of the pore ordering. As it was reported by Meinen, *et al*. [31] the XRD pattern for MCM-41 contains four main reflection lines at low angles, as can be observed in Figure 14.

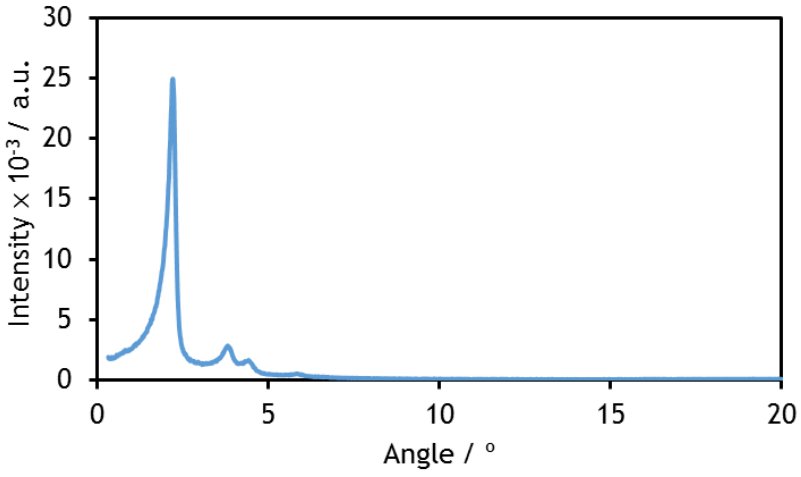

Figure 14 – XRD pattern of MCM-41 powder.

Helium picnometry and mercury intrusion porosimetry tests were used to characterize the granulates and the results are presented in Table 2.

Table 2 - Helium picnometry and Mercury intrusion porosimetry results.

Helium Picnometry	
Solid Density ($g \cdot ml^{-1}$)	1.68
Mercury Porosimetry	
Total Intrusion Volume ($ml \cdot g^{-1}$)	0.78
Median Pore diameter (Volume) (nm)	127
Bulk Density ($g \cdot ml^{-1}$)	0.59
Apparent Density ($g \cdot ml^{-1}$)	1.08
Porosity (%)	45.6

From the nitrogen adsorption isotherms at 77 K for powder and granulates (Figure 15) it was possible to understand that the adsorbent loses some adsorption capacity during the shaping procedure.

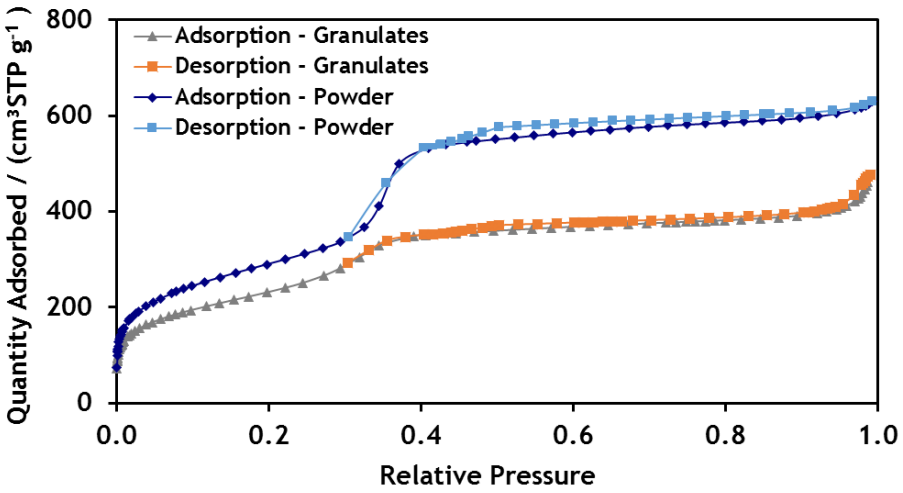

Figure 15 – N_2 isotherms for the powder and granulates.

The obtained pore volume and BET surface areas for both samples are shown in Table 3.

Table 3 – Pore Volume and BET Surface Area of the powder and granulates.

	Pore volume ($cm^3 \cdot g^{-1}$)	**BET Surface Area ($m^2 \cdot g^{-1}$)**
Powder	0.97	1059
Granulates	0.74	844

3.4 Adsorbent regeneration

To regenerate the adsorbent were performed several tests in order to understand which regeneration procedure is the most efficient. First, it was used water at ambient temperature and warm/hot water. It was noticed that in both tests the regeneration was not possible. Juang *et al.*[32] proposes the use of an acid or a base, such as a hydrochloric acid or sodium hydroxide as regeneration method. It turned out that this method was not efficient and that the adsorbent is soluble in the base. It was also tested the use of pure acetone and ethanol and the regeneration was neither achieved.

It was found in the literature an example of regeneration of a mesoporous silica adsorbent, with acetone and hydrochloric acid which has been effective [33]. Therefore, it was tested with the adsorbent MCM-41 the regeneration with a mixture of acetone, water and hydrochloric acid and the regeneration was almost 100% efficient. The composition of the regeneration mixture used is, for a volume of 170 ml, 100 ml of acetone, 50 ml of water and 20 ml of hydrochloric acid with 0.5 M concentration.

3.5 Adsorption equilibrium isotherms

The adsorption equilibrium data can be assessed through batch mode measurements, by obtaining the concentration in both adsorbent and adsorbate at a constant temperature. The experimental results can be compared with theoretical models, such as the Langmuir, Freundlich, Sips and others.

The first is represented by [34]:

$$q = \frac{Q_m K_L c}{1 + K_L c} \tag{3.1}$$

Where q represents the adsorbed amount at the equilibrium, c is the solution equilibrium concentration and the parameters Q_m and K_L represent the maximum adsorption capacity and a constant related to the free energy of adsorption, respectively.

The Freundlich model is represented by [34]:

$$q = K_F c^{1/n} \tag{3.2}$$

Where the parameter K_F represents the Freundlich isotherm constant, which is an indicative of the extent of adsorption and $1/n$ represents the adsorption intensity.

The Sips equation, also called the Langmuir-Freundlich equation, once it results from a combination of both is represented by [34]:

$$q = \frac{Q_m K_L c^n}{1 + K_L c^n} \tag{3.3}$$

The multicomponent adsorption can be predicted using the extended models. The extended Langmuir equation is represented by:

$$q = \frac{Q_{m_i} K_{L_i} c_i}{1 + \sum_{j=1}^{n} K_{L_j} c_j} \tag{3.4}$$

The extended Sips equation is represented by:

$$q = \frac{Q_{m_i} K_{L_i} {c_i}^{n_i}}{1 + \sum_{j=1}^{n} K_{L_j} {c_i}^{n_j}} \tag{3.5}$$

The adsorption equilibrium isotherms were obtained for the selected dyes: Methylene Blue, Basic Blue 41, Basic Red 18, Reactive Red 239 and Orange II. The tests were conducted in Erlenmeyer flasks and it was used a volume of 150 ml of Methylene Blue and Orange II with a concentration of 10 mg·l^{-1}. For Reactive Red 239 and Basic Blue 41 a volume of 200 ml was used with an initial concentration of 20 mg·l^{-1}. Finally, for the Basic Red 18 was used an initial concentration of 20 mg·l^{-1} and a volume of 150 ml. Besides the individual compounds, it were also performed essays in order to obtain binary adsorption equilibrium data. So for the mixture of Basic Blue 41 ad Basic Red 18 it was used an initial concentration of 20 mg·l^{-1} for each dye and a total volume of 150 ml.

These flasks were agitated in order to promote the contact between the solution and the adsorbent. After one week, the absorbance of the mixture was measured with the spectrophotometer at the maximum wavelength for each dye.

3.6 Adsorption kinetics

Kinetics essays were performed with the aim of understanding possible kinetic limitations. Therefore, to perform the essays, a batch reactor with a thermal bath was used in order to assure a constant temperature, in this case 20 ºC. The reactor was filled with a solution volume of 200 ml and that solution was kept agitated. The tests were performed as long as necessary to achieve the adsorption equilibrium. The unit scheme is presented in Figure 16. These essays were only performed with the cationic dyes once it was already concluded that the anionic dyes does not adsorb on MCM-41.

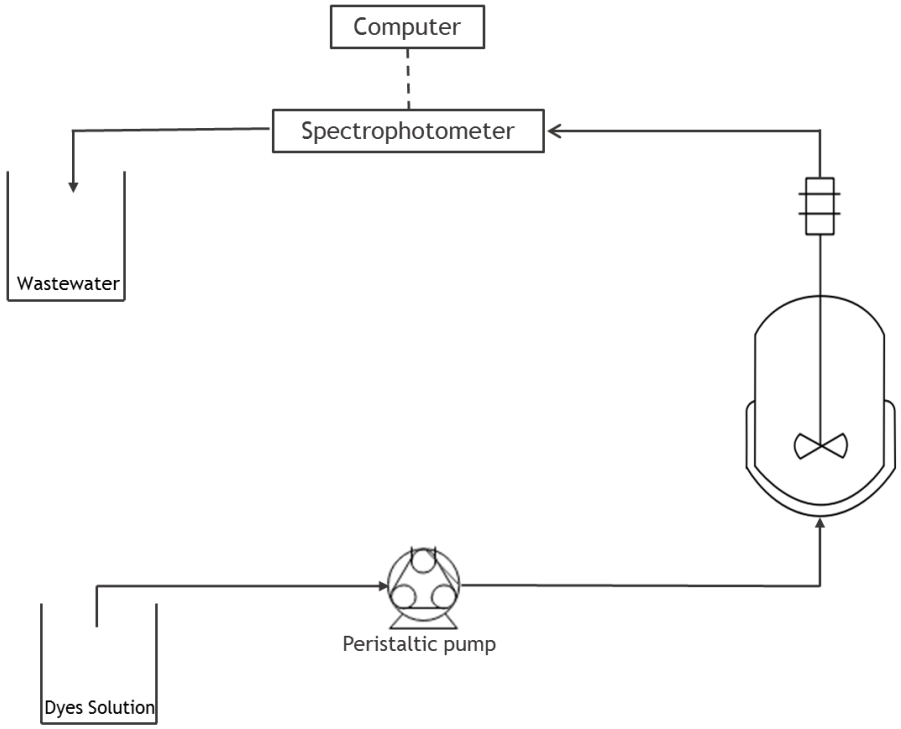

Figure 16 – Unit scheme for batch experiments.

3.7 Fixed bed adsorption

3.7.1 Breakthrough Curves

Fixed bed experiments were performed in a packed column. Breakthrough curves were obtained for dyes Basic Blue 41 and Basic Red 18. Flow rates of 1.29 ml·min^{-1} and 0.85 ml·min^{-1} were used for each dye, respectively with a feed concentration of 20 mg·l^{-1}. The bed height used was 3.5 cm and the column diameter 7 mm. Desorption experiments were also performed in order to obtain the breakthrough curves for the adsorbent regeneration.

The unit scheme for breakthrough experiments is presented in Figure 17.

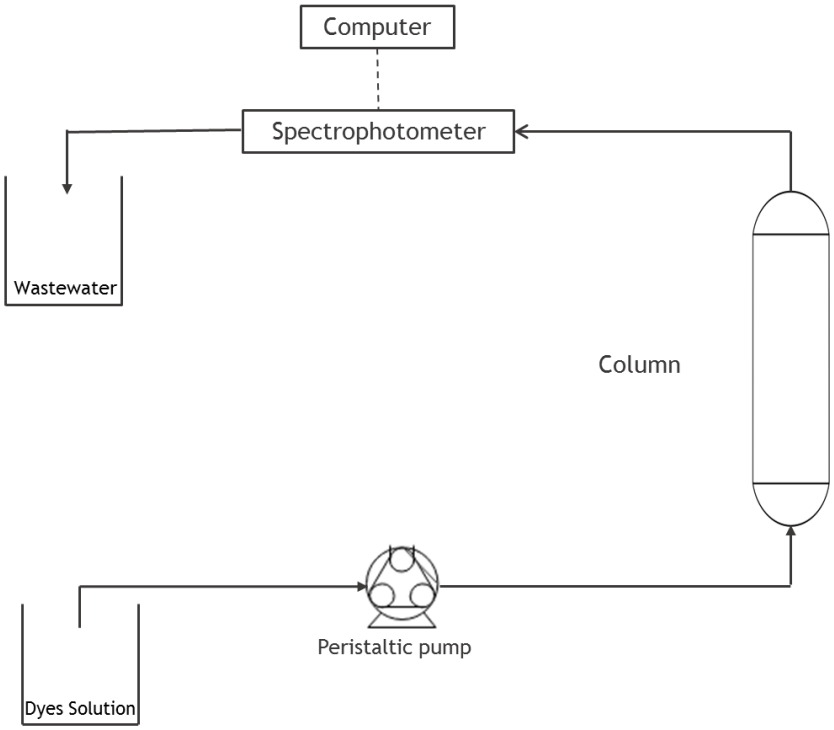

Figure 17 – Unit Scheme for breakthrough experiments.

From breakthrough curves, it is possible to calculate the breakthrough time, the stoichiometric time and the capacity of the column.

The stoichiometric time is given by

$$t_{st} = \int_0^t \left(1 - \frac{C}{C_\infty}\right) dt \tag{3.6}$$

Being the C_∞ the equilibrium concentration, equal to the feed concentration.

The capacity of the column, the maximum adsorbed amount, is given by

$$q = \frac{C_\infty Q \int_0^t \left(1 - \frac{C}{C_\infty}\right) dt - \varepsilon V C_\infty}{m_{ads}} \tag{3.7}$$

where Q is the flow rate, ε is the porosity, V is the column volume and m_{ads} is the mass of the adsorbent in the column.

3.7.2 Pulse experiments

In order to evaluate the separation of two dyes, pulse experiments were taken in a column with dyes differently charged. The unit scheme is presented in Figure 18. A loop of 2 ml was used and the dye solution is a mixture of two dyes, a cationic dye, Basic Blue 41 and an anionic dye, Orange II. The concentration used was 40 mg·l^{-1} and 20 mg·l^{-1}, respectively. A metallic column

and metallic tubes were used in order to minimize the adsorption of the cationic dye on the silicon tubing. The flowrate used was about 5 ml·min^{-1}, with a velocity of the peristaltic pump of 20 rpm.

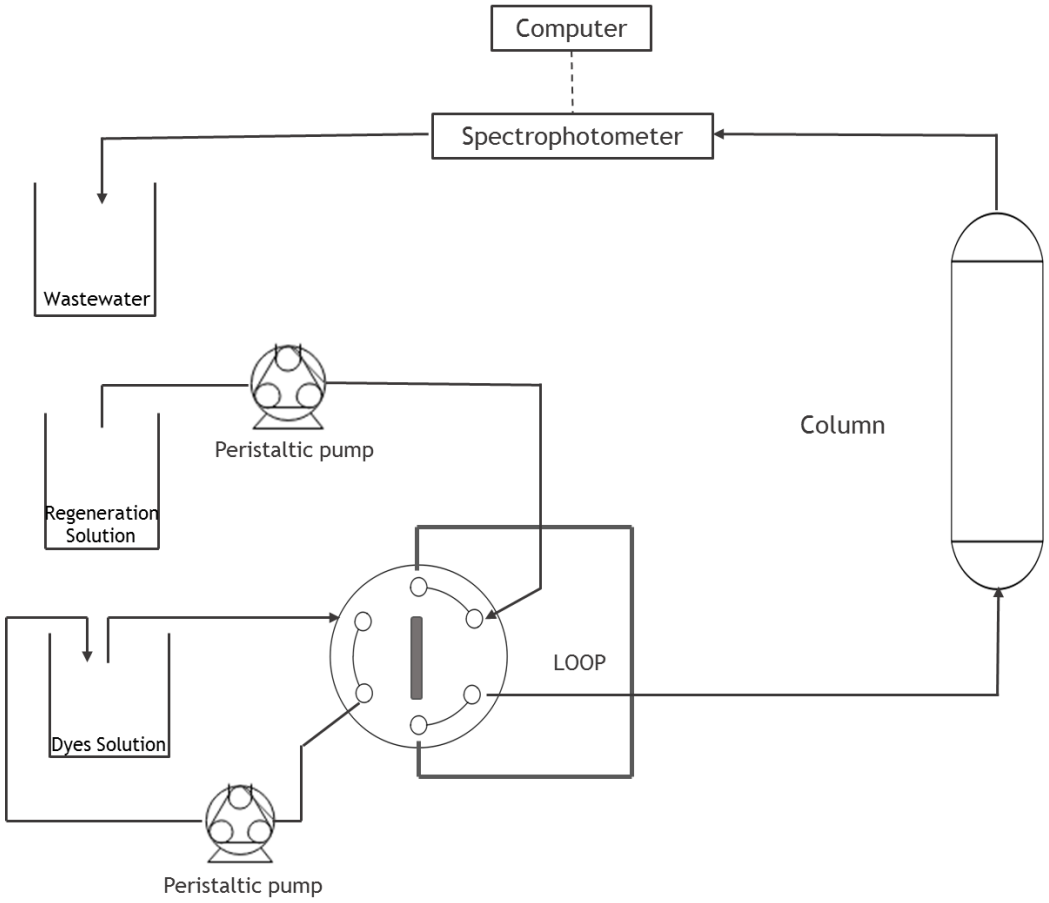

Figure 18 – Unit Scheme for impulse experiments.

3.8 Chromatography

Chromatography is a physical method of separation in which components from a sample are distributed between two phases: the stationary phase and the mobile phase. The stationary phase may be a solid, a gel or a liquid, while the mobile phase may be a liquid, a gas or a supercritical fluid [27].

The chromatographic system is constituted by four parts: a device for sample introduction, a mobile phase, a stationary phase and a detector.

3.9 Ultraviolet-Visible (UV-Vis) Spectroscopy

The ultraviolet region comprises wavelengths between 190-380 nm and the visible region, wavelengths between 380-750 nm. These higher energy radiations causes many molecules to suffer electronic transitions. The principle of operation consists on a radiation with a range of wavelengths that is passed through a sample and the transmittance is measured. Absorbance can be calculated as $A = -\log(T)$ [27,28].

UV-Vis Spectroscopy can be used in a qualitative way, to identify functional groups or compounds, or in a quantitative way, to obtain the concentration of an analyte, which is related to the absorbance [29]. The Beer-Lambert Law relates the concentration to the absorbance by

$$A = \varepsilon\, l\, c \tag{3.8}$$

being ε the molar absorptivity, *c* the concentration of the solution and *l* the length of the light path [30].

This method was selected in order to follow or obtain the dye concentration in this manuscript. Jenway 6305 spectrophotometer, UK was used.

4 Results and Discussion

4.1 Equilibrium isotherms

4.1.1 Single component adsorption

In Figure 19 are presented all of the experimental points of the adsorption equilibrium isotherms.

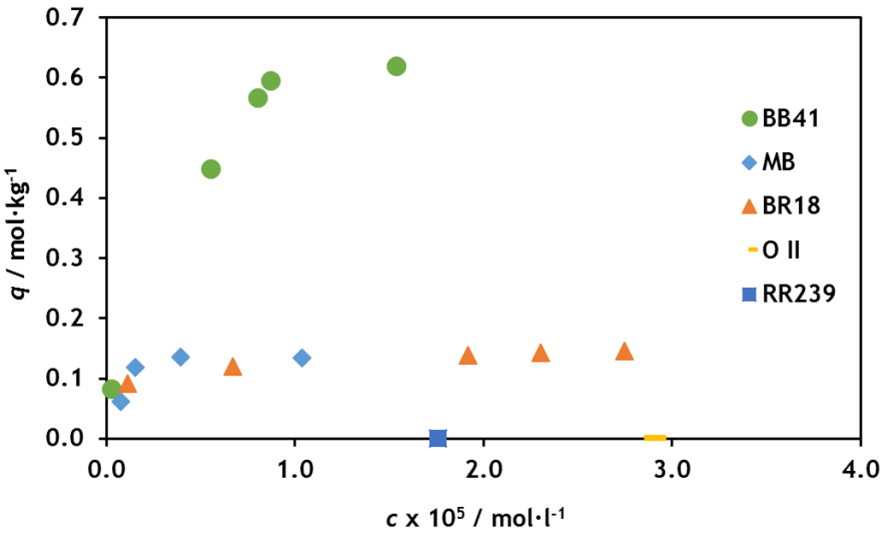

Figure 19 – Isotherms experimental points.

For anionic dyes, Reactive Red 239 and Orange II it was possible to conclude that these dyes do not adsorb in the MCM-41 adsorbent as it was already explained.

For the cationic dyes were obtained the isotherms represented in Figure 20, Figure 21 and Figure 22. In these figures it is also represented the Langmuir, Freundlich and Sips models regressed against the experimental points.

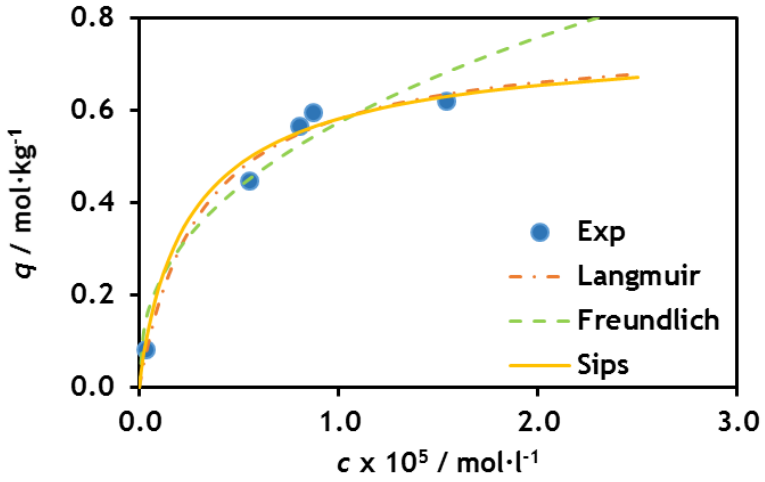

Figure 20 - Experimental points and adjustment curves for the dye Basic Blue 41.

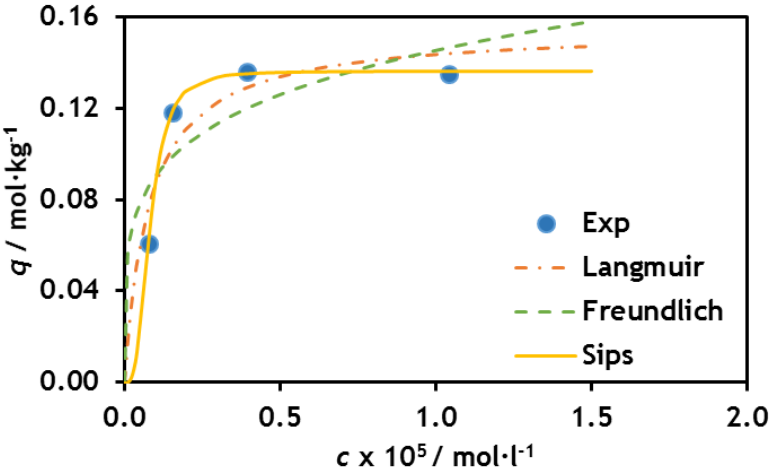

Figure 21 - Experimental points and adjustment curves for the dye Methylene Blue.

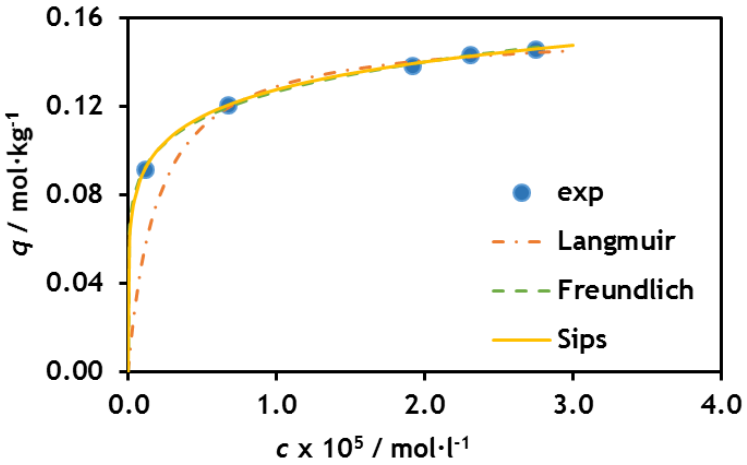

Figure 22 - Experimental points and adjustment curves for the dye Basic Red 18.

From the observation of the presented models, it is possible to conclude that the model that best describes the equilibrium isotherms is the Sips model for all dyes. Otherwise, the Basic

Blue 41 isotherm is closer to the Langmuir form and the Basic Red 18 to the Freundlich isotherm. The parameters of the three models are presented in Table 4.

Table 4 - Langmuir, Freundlich and Sips isotherm parameters.

Dye	Model						
	Langmuir		Freundlich		Sips		
	Q_m (mol·kg^{-1})	K_L (l·mol^{-1})	K_F (mol·kg^{-1}· (l·mol^{-1})$^{1/n}$)	n	Q_m (mol·kg^{-1})	K_L ((l·mol^{-1})^n)	n
Basic Blue 41	0.77	3.19	0.57	2.48	0.79	2.84	0.90
Methylene Blue	0.15	12.74	0.15	4.85	0.14	2005	3.04
Basic Red 18	0.16	5.00	0.13	6.89	0.33	0.62	0.23

The three isotherms and the respective Sips model are presented in Figure 23. From the comparison of the isotherms, it is possible to conclude that the dye Basic Blue 41 adsorbs more than the other two dyes in the studied range of concentrations.

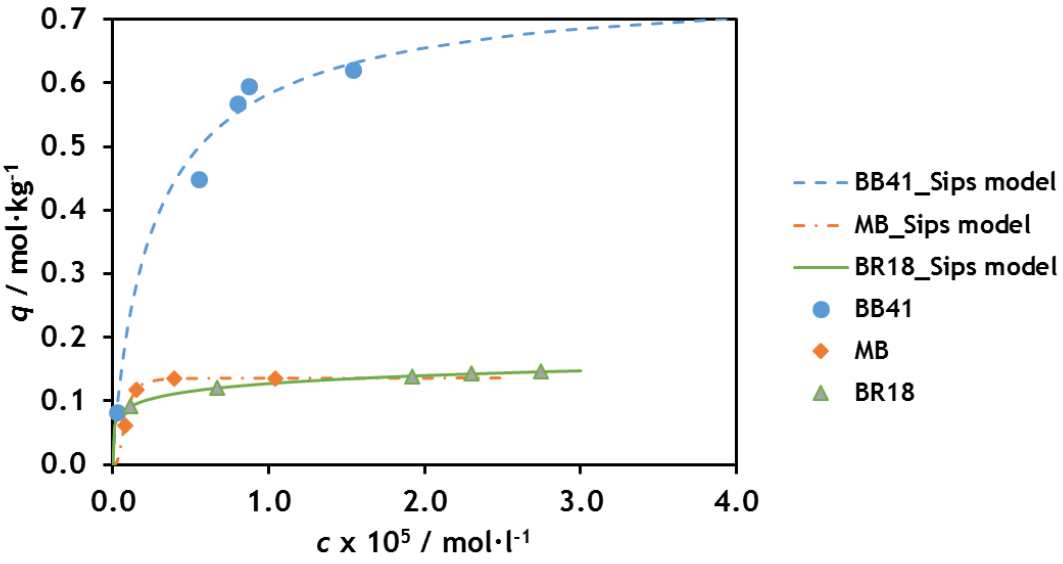

Figure 23 - Isotherms and its best adjustment.

4.1.2 Multicomponent adsorption

In Figure 24 and Figure 25 are presented the binary adsorption equilibrium points obtained experimentally for the dyes Basic Blue 41 and Basic Red 18. Additionally, the experimental results are compared with the predictions obtained using the multicomponent Langmuir and Sips extended equations.

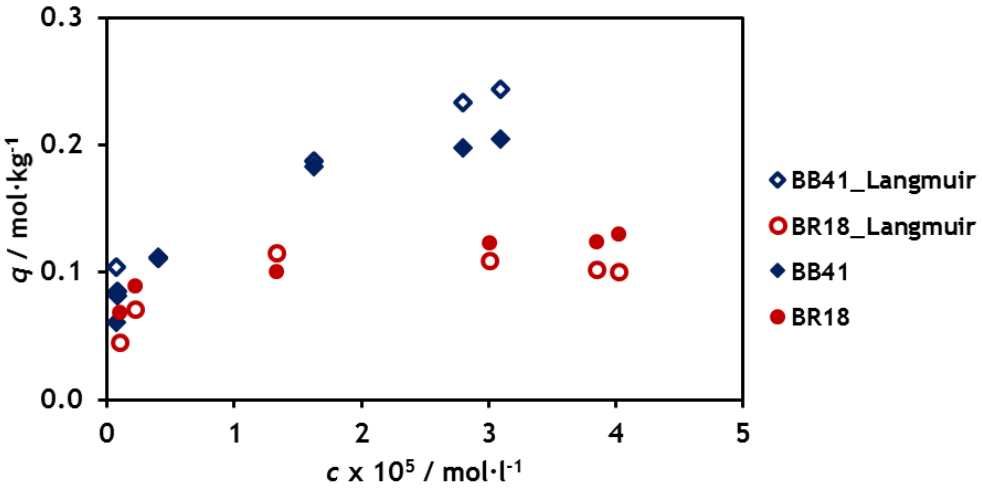

Figure 24 – Multicomponent experimental points multicomponent Langmuir extension adjustment.

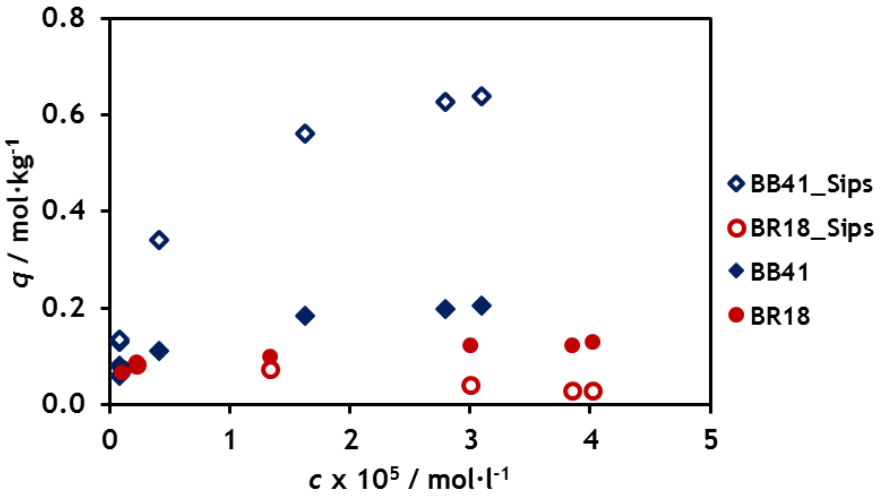

Figure 25 - Multicomponent experimental points multicomponent Sips extension adjustment.

In Table 5 are presented the previous results in form of a table. Although, the single component adsorption is better fitted with the Sips model; for binary adsorption equilibrium, the extended Langmuir equation represents better the experimental adsorption binary points.

Table 5 – Multicomponent equilibrium points obtained and expected by the models.

Points	Basic Blue 41				Basic Red 18			
	c x10^5 (mol·l^{-1})	q (mol·kg^{-1})	$q_{Langmuir}$ (mol·kg^{-1})	q_{Sips} (mol·kg^{-1})	c x10^5 (mol·l^{-1})	q (mol·kg^{-1})	$q_{Langmuir}$ (mol·kg^{-1})	q_{Sips} (mol·kg^{-1})
1	0.07	0.06	0.10	0.13	0.10	0.07	0.04	0.07
2	0.08	0.08	0.085	0.14	0.22	0.09	0.07	0.08
3	0.41	0.11	0.11	0.34	1.33	0.10	0.12	0.08
4	1.63	0.18	0.19	0.56	3.00	0.12	0.11	0.04
5	2.79	0.20	0.23	0.63	3.85	0.12	0.10	0.03
6	3.09	0.20	0.24	0.64	4.02	0.13	0.10	0.03

4.2 Adsorption kinetics

In Figure 26 and Figure 27 are presented the normalized concentration and the adsorbed amount in function of time, respectively. It is possible to observe that adsorption kinetics is faster for the dye Basic Blue 41 since it reaches the equilibrium quicker than the other two basic dyes, Methylene Blue and Basic Red 18.

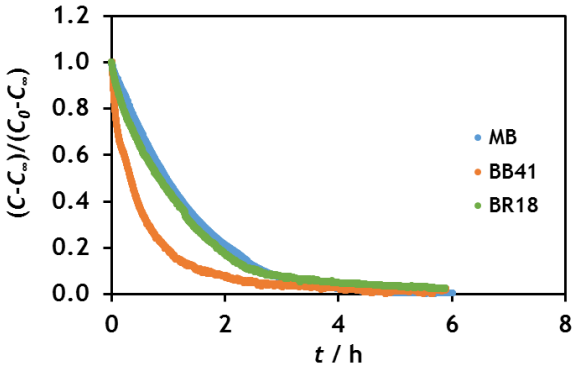

Figure 26 – Normalized concentration vs time for the three dyes.

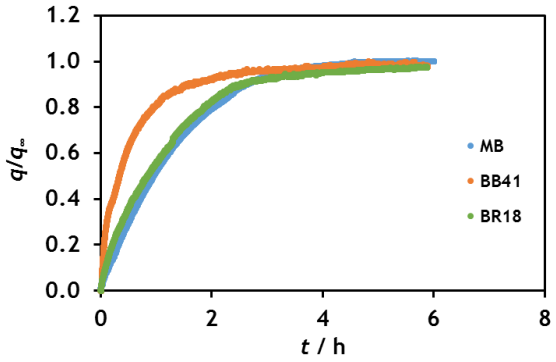

Figure 27 – Normalized adsorbed amount vs time for the three dyes.

In *Figure 28* and *Figure 29* are presented the kinetic tests for the dye Basic Blue 41 with the fresh adsorbent and the regenerated adsorbent. From the analyses, it is possible to find out that the adsorption is faster in the fresh adsorbent.

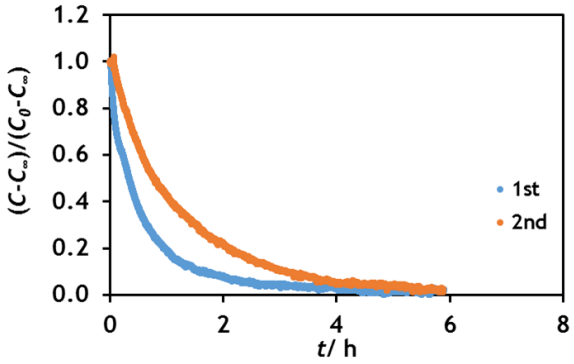

Figure 28 – Normalized concentration vs time for the fresh adsorbent and the regenerated one.

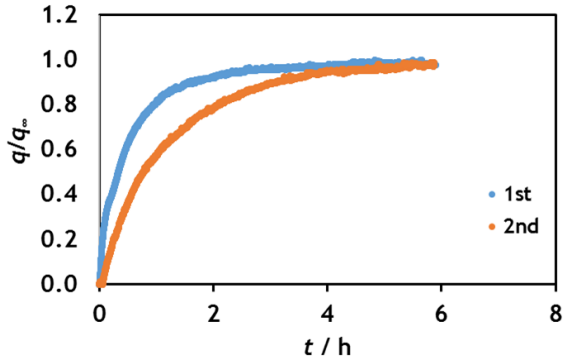

Figure 29 - Normalized adsorbed amount vs time for the fresh adsorbent and the regenerated one.

It were also performed essays in order to evaluate the desorption kinetics and are presented in Figure 30 and in Figure 31 for two cationic dyes, Methylene Blue and Basic Blue 41. It is noticed that de desorption process in this case is much faster than the adsorption, lasting less than 1 hour, while adsorption takes more or less 6 hours.

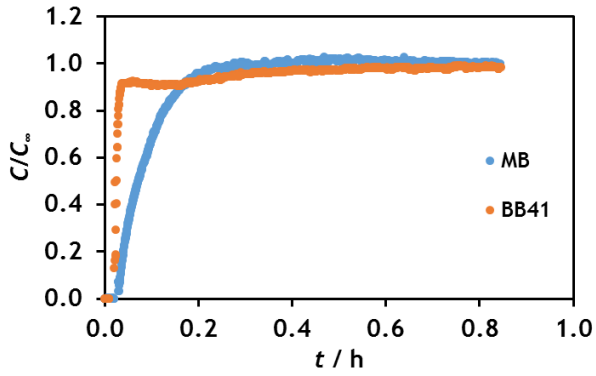

Figure 30 – Normalized concentration vs time for the desorption of the dyes.

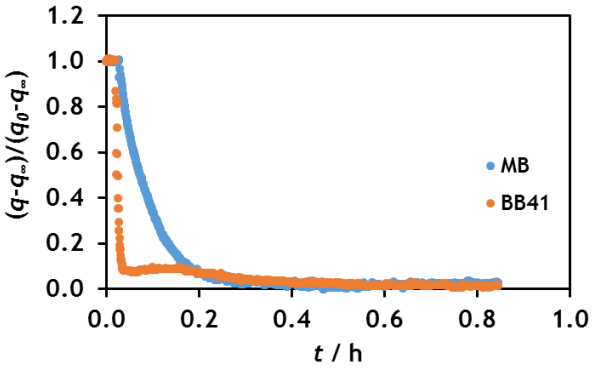

Figure 31 – Normalized adsorbed amount vs time for the desorption of the dyes.

The results of all performed experiments are presented in Appendix 3.

4.3 Breakthrough Curves

In Figure 32 is presented the breakthrough curve for the dye Basic Blue 41 in MCM-41 adsorbent. While the breakthrough curve of Basic Blue 41 desorption is presented in Figure 33.

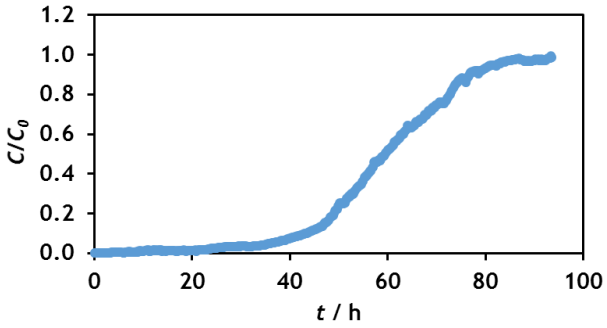

Figure 32 - Breakthrough curve for the dye Basic Blue 41.

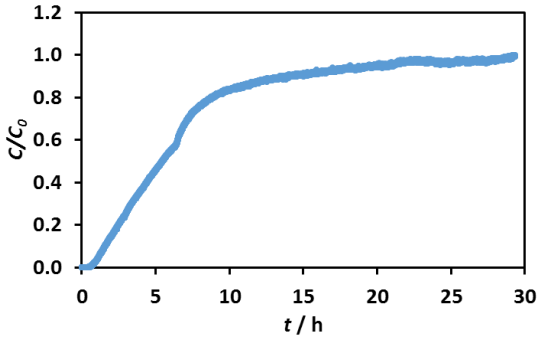

Figure 33 – Breakthrough curve for the desorption of the dye Basic Blue 41.

The breakthrough curves of the adsorption and desorption of the dye Basic Red 18 are presented in Figure 34 and Figure 35, respectively.

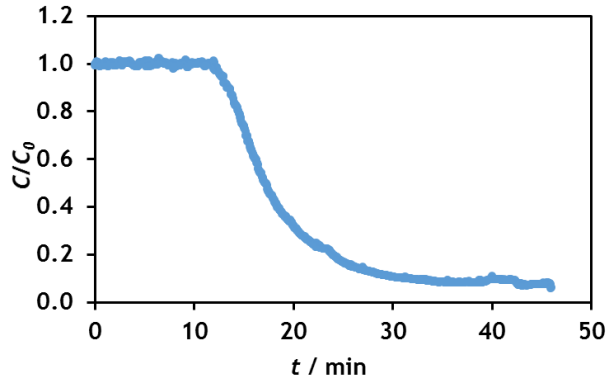

Figure 34 – Breakthrough curve for the dye Basic Red 18.

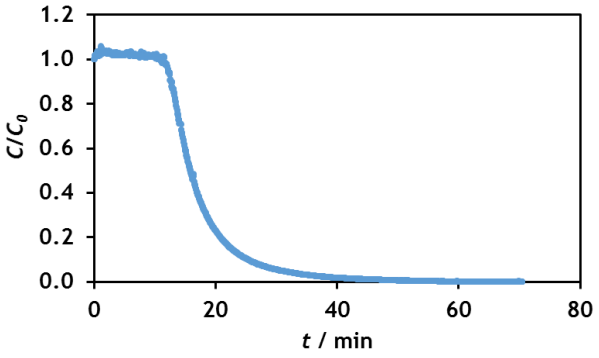

Figure 35 – Breakthrough curve for the desorption of the dye Basic Red 18.

The capacity of the column was calculated by the integration of the breakthrough curves. It was also possible to estimate the stoichiometric and the breakthrough times. These results are presented the Table 6.

Table 6 – Adsorbed quantity, stoichiometric time and breakthrough time.

Dye	q (mg·g^{-1})	q (mol·kg^{-1})	t_{st} (h)	t_{Bp} (h)
Basic Blue 41	189	0.39	60	36
Basic Red 18	14	0.03	7	1

From the analyses of breakthrough curves and the estimated parameters it is possible to check that adsorbed quantity is much higher for the dye Basic Blue 41 than for the dye Basic Red 18, as it was already expected, from the adsorption equilibrium isotherms results. Besides that, the adsorbed quantity obtained in these experiments is lower than the one estimated through the isotherms models. This was already expected once, as it was already mentioned, the obtained granulates adsorb less than the powder, which was used to determine the isotherms. The calculated adsorbed quantity for the Basic Red 18 is much lower than what is expected from the adsorption equilibrium isotherm, it is probably due to the regeneration of the adsorbent which was not performed properly. This essay must be repeated in order to verify the results.

Relatively to the desorption breakthrough curves can be concluded that the adsorbent was almost fully regenerated in less than one hour for both dyes.

4.4 Pulse experiments

In Figure 36 are presented the curves of the chromatographic separation of dyes Basic Blue 41 and Orange II in a column. The graph shows the curves in the maximum wavelengths of both dyes. When following the 590 nm wavelength, only one peak is observed, corresponding to the Basic Blue 41 (Orange II does not absorb light at this wavelength). When following the 483 nm wavelength it appears two peaks, one corresponding to the Orange II, that hardly adsorbs on MCM-41 and therefore its retention time is almost identical to the space time of the column. While the second peak, as can clearly be observed, corresponds to Basic Blue 41 that absorbs light on this wavelength to a lower extent.

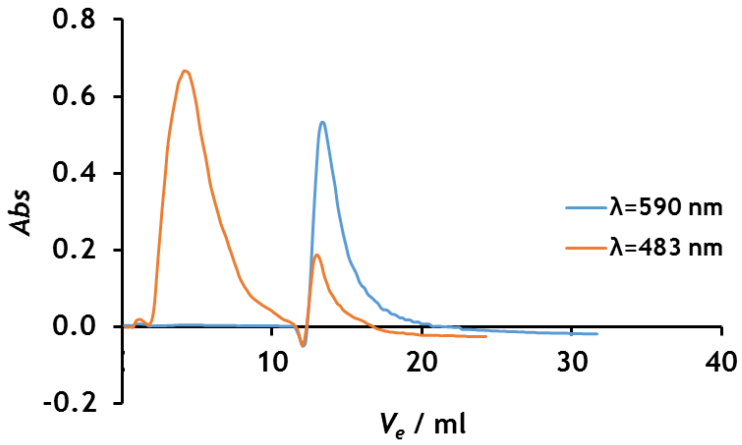

Figure 36 – Pulse response curves in the column experiment in both wavelengths.

In Figure 37 are presented, the original mixture solution (green) and collected fractions Orange II and Basic Blue 41.

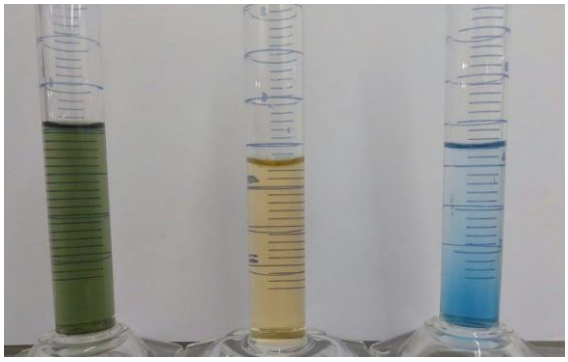

Figure 37 – Graduated tubes with the original mixture solution (green), collected Orange II and Basic Blue 41.

In order to evaluate if the adsorption process is only taken on the adsorbent, tests with a column filled with metallic spheres and only the tubes (blank tests) were performed. The last one also allowed to understand the dead volume, time corresponding to the tubing. From Figure 38 it is possible to understand that the adsorption in the tubes is negligible compared with the adsorption in the adsorbent. On the other hand, the blank test in the column filled with the metal spheres, presented in Figure 39, shows that Basic Blue 41 still adsorbs significantly in other supposedly *"inert"* materials. The material responsible for this might be the glass wool in the top of the column. All obtained results are presented in the Appendix 4.

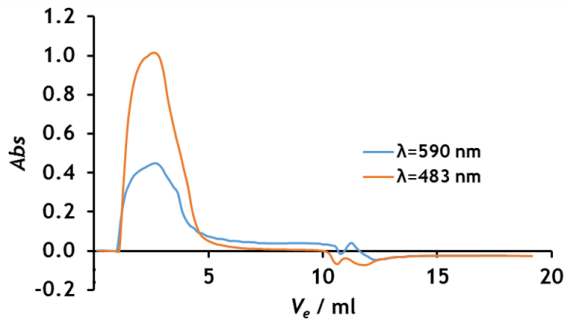

Figure 38 – Pulse response curves in the tubes.

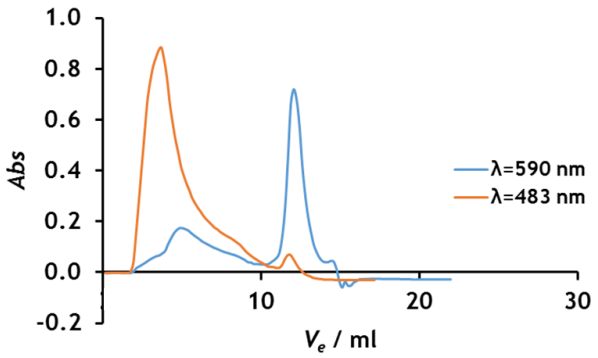

Figure 39 – Pulse response curves in the column filled with metallic spheres.

4.5 Interaction between cationic and anionic dyes

It was noticed during the tests done that the Beer-Lambert rule was failing when applied to mixtures of dyes with different charge since the absorbance of a mixture was not corresponding to the sum of the pure component absorbance for all wavelengths (see Figure 40).

It was used a scanning spectrometer in order to obtain the representation of the absorbance in all wavelengths. The dyes used were Methylene Blue and Orange II with different concentrations. For the analysis, it was calculated the expected absorbance of the mixture by adding the pure dyes spectra for the different concentrations. The highest studied concentration, 10 $mg \cdot l^{-1}$ for both dyes, spectra is represented in Figure 40. It can be understood that the mixture of the dyes generate an absorbance lower than what is expected, according to the Beer-Lambert law.

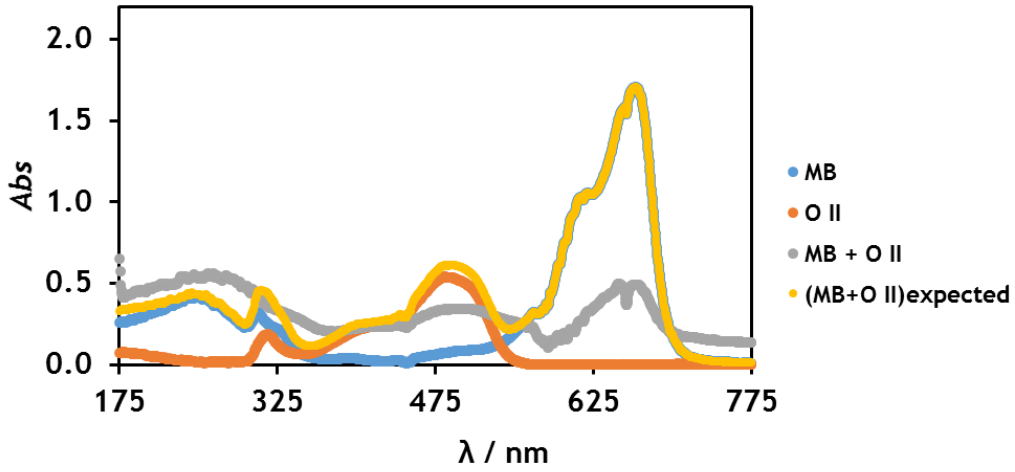

Figure 40 - Spectra of Methylene Blue and Orange II for a concentration of 10 $mg \cdot l^{-1}$.

This can be explained because of the interactions between the two different charge species leading to the formation of a complex, originating a lower concentration of both dyes in the solution. The complex formation it was already observed in the literature with two other different dyes, Basic Blue 9 (Methylene Blue) and Acid Blue 25 [35]. Additionally, after letting the mixture resting some time it was possible to observe the deposition of a solid (see Figure 41).The absorbance of the supernatant mixture is presented in Figure 42. From Figure 42 can be concluded by the direct comparison of the curves in the graph that the absorbance of the supernatant solution is lower and the complex absorbs light equally in all wavelengths. Indeed, its presence only generates an increase of the spectra base line.

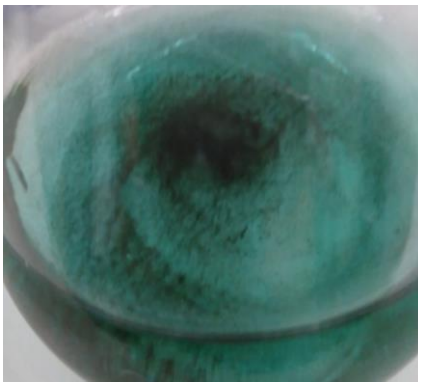

Figure 41 – Dye complex formed.

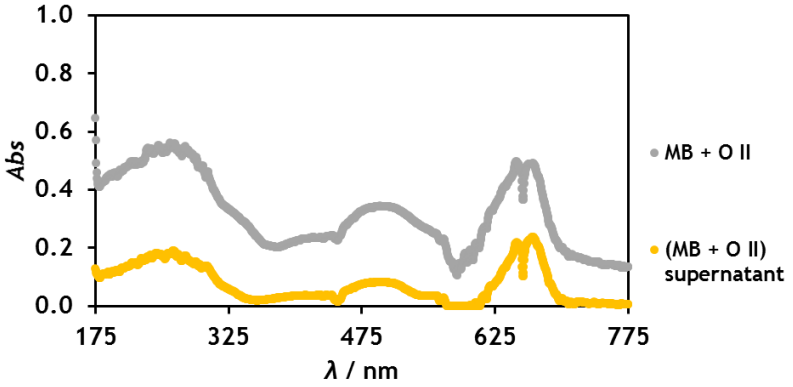

Figure 42 – Spectra of Methylene Blue and Orange II with and without the complex.

To understand if the complexation reactions only occur in the presence of dyes with opposite charges, a spectrum for the mixture of the cationic dyes Basic Blue 41 and Basic Red 18 was also obtained. Spectra for a concentration of 20 $mg \cdot l^{-1}$ for both dyes and the mixture is presented in Figure 43.

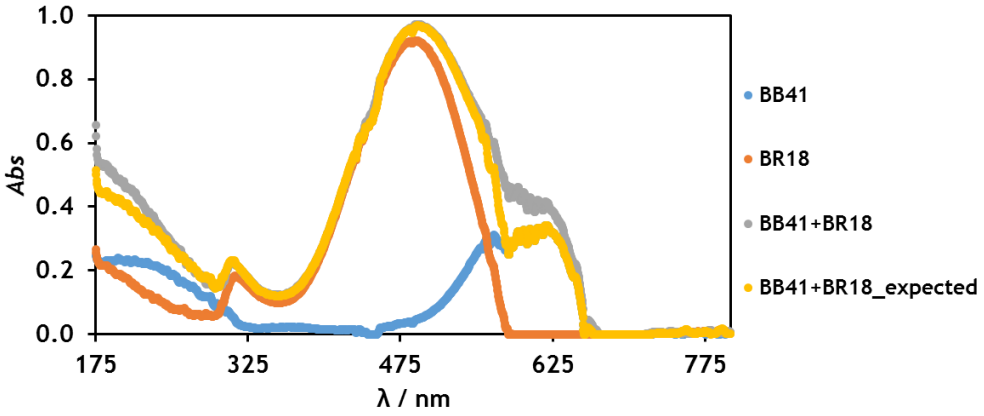

Figure 43 - Spectra of Basic Blue 41 and Basic Red 18 for a concentration of 20 $mg \cdot l^{-1}$.

From the obtained spectra, it was possible to conclude that the absorbance of the mixture is the sum of the pure component spectra for all wavelengths, such is possible to visualize when comparing the grey and yellow curves, which represent the real absorbance of the mixture and the predicted absorbance, respectively.

5 Experimental protocol

Verify if the installation is set up as the scheme presented in Figure 44.

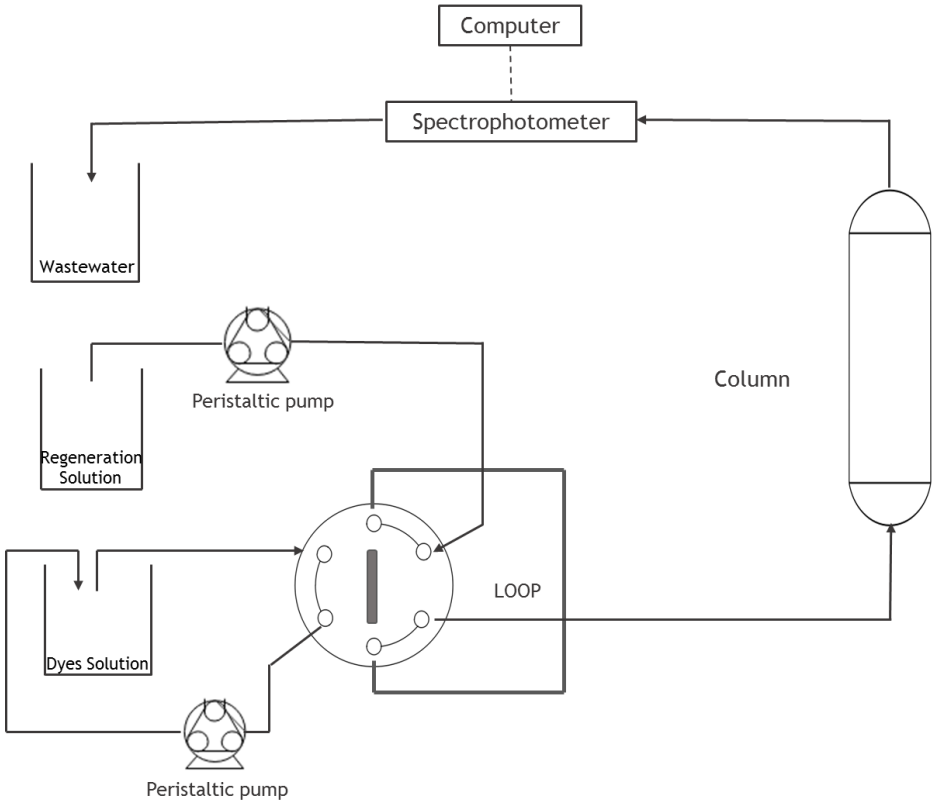

Figure 44 – Experimental unit at the loading position.

Turn on the spectrophotometer and wait until it get ready. Select the maximum wavelength of one of the dyes, 590 nm for the Basic Blue 41 and 483 nm for Orange II. Turn on the computer and open the LabVIEW interface that allows recording the absorbance reading from the spectrophotometer.

Then prepare the regeneration solution and the dyes mixture solution. The first one, for a volume of 170 ml, mix 50 ml of distilled water, 100 ml of acetone and 20 ml of hydrochloric acid, 0.5 M concentration. The dyes mixture solution is prepared from the concentrated solutions available, in order to obtain a concentration of 40 $mg \cdot l^{-1}$ of Basic Blue 41 and 20 $mg \cdot l^{-1}$ of Orange II. This solution should be prepared just before the experiment to minimize the formation of a complex between the two dyes.

After preparing the solutions, it is necessary to calibrate the spectrophotometer. So turn on the peristaltic pump, set it to a flowrate of about 5 $ml \cdot min^{-1}$, and pass distilled water through the tubes, column and the cell of the spectrophotometer.

While the calibration is done, it is possible to fill the loop with the dyed solution. So turn on the other peristaltic pump with the same flowrate and wait until the loop is filled.

Then, it is possible to start the experiment, changing the feed from the water flask to the regeneration solution flask. At the same time start saving the data through the program and rotate the loop valve to the position represented in Figure 45.

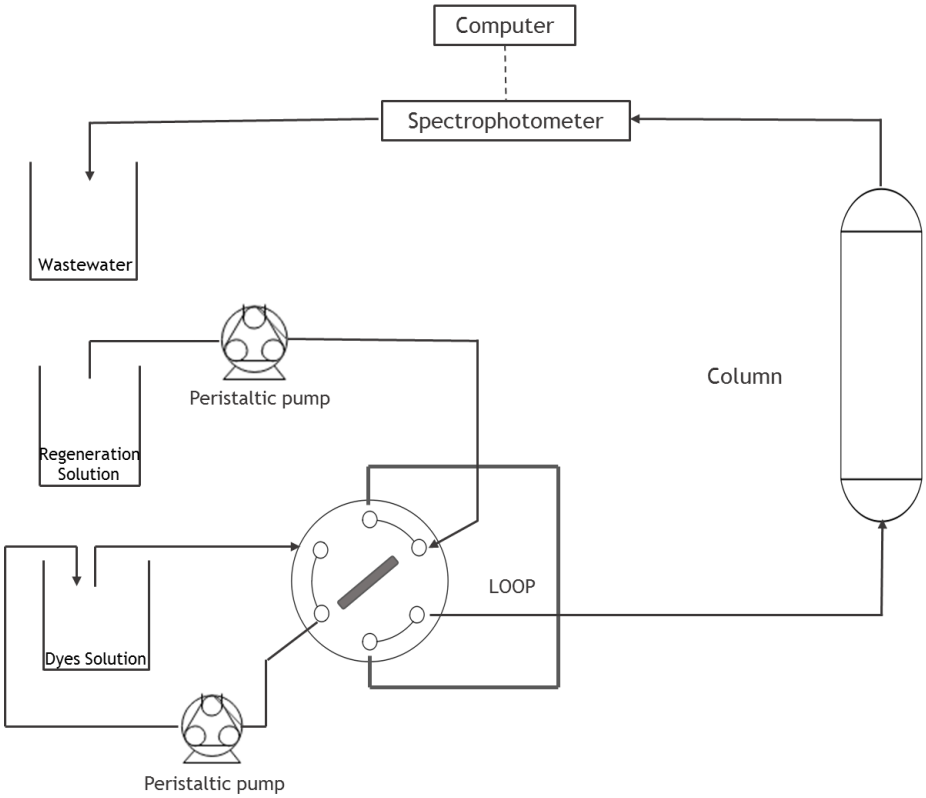

Figure 45 - Experimental unit at the injection position.

After the loop is empty of the dye solution, rotate the valve back to the initial position. This step is important to avoid the cleaning of the loop tube with the regeneration solution.

Measure the flowrate during the experiment.

Take the experiment until the adsorbent is regenerated, that is, the absorbance reaches a baseline correspondent to the regenerating solution.

When it finishes pass water as in the beginning and repeat the experiment with the second wavelength.

6 Conclusions

The adsorbent selected was MCM-41, due to its high surface areas and high pore volumes, which would lead to a high adsorption capacity. Besides that, this adsorbent has the property of only adsorbing cationic compounds due to its surface chemistry.

The adsorption equilibrium isotherms were regressed against three models, Langmuir, Freundlich and Sip. The one that better describes the adsorption equilibrium was the Sips model for the three dyes tested Basic Blue 41, Basic Red 18 and Methylene Blue. It was also concluded that the adsorbent adsorbs a higher quantity of Basic Blue 41 than the other two dyes.

Batch experiments were performed in order to evaluate if there were kinetics limitations and it was concluded that the adsorption kinetics is slow for all dyes in the adsorbent. However, Basic Blue 41 dye has a faster adsorption kinetics compared with the other two dyes Basic Red 18 and Methylene Blue. One the other hand the regeneration was much faster when compared with the adsorption process.

The breakthrough tests showed that the adsorption capacity for dyes Basic Blue 41 and Basic Red 18 are 189 $mg \cdot g^{-1}$ and 14 $mg \cdot g^{-1}$, respectively.

As an objective to separate dyes in a fixed bed column experiment, pulse experiments were performed with a binary mixture of dyes opposite charged, Basic Blue 41 and Orange II. It was possible to observe two peaks leaving the column in different times, corresponding the first peak to the anionic dye, which is not retained in the adsorbent, being the time that it leaves the column equal to the space time of the system. The second peak corresponds to the cationic dye which is retained in the adsorbent and only leaves the column with the regeneration solution.

It was concluded that it was not possible to quantify the concentration of the components in a binary mixture with dyes differently charged once the Beer-Lambert rule cannot be applied because the absorbance of the mixture of dyes does not correspond to the sum of pure component absorbance. This results as a consequence of the formation of an ionic complex which causes a minor concentration of the dyes in the mixture.

7 Assessment of the work done

7.1 Objectives Achieved

One of the objectives was testing capacity of a mesoporous silica based adsorbent in wastewater treatment. This objective was achieved once breakthrough tests were performed and it was noticed that the chosen adsorbent has a high adsorption capacity for cationic dyes.

Another objective was the chromatographic separation of a mixture of dyes in a fixed bed column. This objective was reached as pulse experiments were performed in a packed column and two fractions were collected with each one of dyes. Furthermore, the required experimental time is adequate to propose such experimental work as a potential work to be included in the curricular plan of *Práticas de Engenharia Química III*.

7.2 Limitations and Future Work

One of the limitations of the work was the fact that the adsorption using this kind of adsorbents, takes a long time.

Another problem occurred was related to the quantification of the concentration of the dyes in a mixture when the dyes are different charged.

For future work can be important to study other type of adsorbents, in order to obtain a quicker separation.

Another issue was understanding how the regeneration of the adsorbent occurs, once it was not deeply studied.

7.3 Final Assessment

My final assessment of this work is positive once the main objectives were accomplished. There are some issues that were not solved because the available time was not enough.

The work performed during the last five months allowed me to consolidate my knowledge about dyes adsorption.

References

[1] M. T. Yagub, T. K. Sen, S. Afroze, and H. M. Ang, "Dye and its removal from aqueous solution by adsorption: A review," *Adv. Colloid Interface Sci.*, vol. 209, pp. 172–184, 2014.

[2] T. Valencia *et al.*, *General introduction to the chemistry of dyes*, vol. 99. 2010.

[3] K. Hunger and A. Wiley-vch, *Industrial Dyes:*, vol. 125, no. 33. 2003.

[4] J. Best, *Colour design ©*. 2012.

[5] M. Clark, *Handbook of textile and industrial dyeing*. 2011.

[6] David R. Waring and Geoffrey Hallas, *The Chemistry and Application of Dyes*. 1990.

[7] R. F, "The Treatment of Industrial Effluents for the Discharge of Textile Dyes Using by Techniques and Adsorbents," *J. Text. Sci. Eng.*, vol. 6, no. 1, pp. 1–9, 2015.

[8] Z. Wang, M. Xue, K. Huang, and Z. Liu, "Textile dyeing wastewater treatment," *Treat. Text. Effl.*, pp. 91–116, 2011.

[9] G. Pei, F. Yu, and L. Zhang, "Comparative Analysis of dyeing wastewater treatment Technology," no. Iccte, pp. 427–430, 2016.

[10] Masitah Hasan, "Dye: Technologies for Colour Removal." [Online]. Available: http://ppkas.unimap.edu.my/home2015/index.php/news/articles/22-dye-technologies-for-colour-removal.

[11] D. D. Do, *Adsorption Analysis: Equilibrium and Kinetics*, vol. 2. 1998.

[12] B. D. Zdravkov, J. J. Čermák, M. Šefara, and J. Janků, "Pore classification in the characterization of porous materials: A perspective," *Cent. Eur. J. Chem.*, vol. 5, no. 4, pp. 1158–1158, 2007.

[13] M. Thommes *et al.*, "Physisorption of gases, with special reference to the evaluation of surface area and pore size distribution (IUPAC Technical Report)," *Pure Appl. Chem.*, vol. 87, no. 9–10, pp. 1051–1069, 2015.

[14] L. F. Giraldo, B. L. López, L. Pérez, S. Urrego, L. Sierra, and M. Mesa, "Mesoporous silica applications," *Macromol. Symp.*, vol. 258, pp. 129–141, 2007.

[15] F. Rouquerol, J. Rouquerol, K. S. W. Sing, P. Llewellyn, and G. Maurin, *Adsorption by powders and porous solids*. 2014.

[16] H. Furukawa, K. E. Cordova, M. O'Keeffe, and O. M. Yaghi, "The Chemistry and Applications of Metal-Organic Frameworks.," *Science*, vol. 9, no. 6149, p. 1230444, 2010.

[17] A. B. Dichiara, S. J. Weinstein, and R. E. Rogers, "On the Choice of Batch or Fixed Bed Adsorption Processes for Wastewater Treatment," *Ind. Eng. Chem. Res.*, vol. 54, no. 34, pp. 8579–8586, 2015.

[18] J. M. Loureiro, "Notes to Processos Separação II," 2013.

[19] T. M. Albayati, A. A. Sabri, and R. A. Alazawi, "Separation of Methylene Blue as Pollutant of Water by SBA-15 in a Fixed-Bed Column," *Arab. J. Sci. Eng.*, vol. 41, no. 7, pp. 2409–2415, 2016.

[20] A. Gürses, Ç. Doğar, M. Yalçin, M. Açikyildiz, R. Bayrak, and S. Karaca, "The adsorption kinetics of the cationic dye, methylene blue, onto clay," *J. Hazard. Mater.*, vol. 131, no. 1–3, pp. 217–228, 2006.

[21] H. Han, W. Wei, Z. Jiang, J. Lu, J. Zhu, and J. Xie, "Removal of cationic dyes from aqueous solution by adsorption onto hydrophobic / hydrophilic silica aerogel," *Colloids*

Surfaces A Physicochem. Eng. Asp., vol. 509, pp. 539–549, 2016.

[22] S. Santos, "Adsorção de corantes têxteis em materiais naturais e residuais de matriz inorgânica," PhD Thesis, U. Porto, Portugal, 2009.

[23] M. A. M. Salleh, D. K. Mahmoud, W. A. W. A. Karim, and A. Idris, "Cationic and anionic dye adsorption by agricultural solid wastes: A comprehensive review," *Desalination*, vol. 280, no. 1–3, pp. 1–13, 2011.

[24] E. Demirbas, M. Kobya, and M. T. Sulak, "Adsorption kinetics of a basic dye from aqueous solutions onto apricot stone activated carbon," *Bioresour. Technol.*, vol. 99, no. 13, pp. 5368–5373, 2008.

[25] H. Chaudhuri, S. Dash, S. Ghorai, S. Pal, and A. Sarkar, "SBA-16: Application for the removal of neutral, cationic, and anionic dyes from aqueous medium," *J. Environ. Chem. Eng.*, vol. 4, no. 1, pp. 157–166, 2016.

[26] W. Konicki, K. Cendrowski, G. Bazarko, and E. Mijowska, "Study on efficient removal of anionic, cationic and nonionic dyes from aqueous solutions by means of mesoporous carbon nanospheres with empty cavity," *Chem. Eng. Res. Des.*, vol. 94, no. August, pp. 242–253, 2015.

[27] R. E. Ardrey, *Liquid Chromatography - Mass Spectrometry: An Introduction*, vol. 1. 2003.

[28] Tim Soderberg, "Ultraviolet and visible spectroscopy." [Online]. Available: https://chem.libretexts.org/Textbook_Maps/Organic_Chemistry_Textbook_Maps/Map%3A_Organic_Chemistry_With_a_Biological_Emphasis_(Soderberg)/Chapter_04%3A_Structure_Determination_I/4.3%3A_Ultraviolet_and_visible_spectroscopy.

[29] "Ultraviolet-Visible (UV-Vis) Spectroscopy." [Online]. Available: http://www.jove.com/science-education/10204/ultraviolet-visible-uv-vis-spectroscopy.

[30] J. Clark and G. Gunawardena, "The Beer-Lambert Law." [Online]. Available: https://chem.libretexts.org/Core/Physical_and_Theoretical_Chemistry/Spectroscopy/Electronic_Spectroscopy/Electronic_Spectroscopy_Basics/The_Beer-Lambert_Law.

[31] V. Meynen, P. Cool, and E. F. Vansant, "Microporous and Mesoporous Materials Verified syntheses of mesoporous materials," *Microporous Mesoporous Mater.*, vol. 125, no. 3, pp. 170–223, 2009.

[32] L. Juang, C. Wang, and C. Lee, "Adsorption of basic dyes onto MCM-41," vol. 64, pp. 1920–1928, 2006.

[33] Alireza Badiei; Arghavan Mirahsani; Afsaneh Shahbazi; Hbibollah Younesi; Mostafa Alizadeh, "Adsorptive Removal of Toxic Dye From Aqueous Solution and Real Industrial Effluent by Tris(2-aminoethyl)amine Functionalized Nanoporous Silica," *Environ. Sci. Technol.*, vol. 33, no. 2, pp. 482–489, 2014.

[34] M. Belhachemi and F. Addoun, "Comparative adsorption isotherms and modeling of methylene blue onto activated carbons," pp. 111–117, 2011.

[35] D. NB and D.-D. S, "Spectrophotometric Investigation of the Interactions between Cationic (C.I. Basic Blue 9) and Anionic (C.I. Acid Blue 25) Dyes in Adsorption onto Extracted Cellulose from Posidonia oceanica," *J. Text. Sci. Eng.*, vol. 6, no. 1, pp. 1–9, 2015.

[36] L. T. Gibson, "Mesosilica materials and organic pollutant adsorption : part A removal from air," no. c, pp. 5163–5172, 2014.

Appendix 1 – Dyes

Table 7 – Examples of dyes and its classification.

Dye	Common name	Anionic	Cationic	Nonionic	Molecular Formula	Molecular Weight (g mol^{-1})
Textile dyes						
Direct Blue 1	Chicago Sky Blue	✓			$C_{34}H_{24}N_6Na_4O_{16}S_4$	992.81
Basic Violet 1	Methyl Violet		✓		$C_{29}H_{28}N_3NaO_7S_2$	617.67
Acid Orange 7	Orange II	✓			$C_{16}H_{11}N_2NaO_4S$	350.33
Basic Violet 3	Crystal Violet		✓		$C_{25}H_{30}ClN_3$	407.98
Basic Blue 9	Methylene Blue		✓		$C_{16}H_{18}ClN_3S$	319.85
Basic Blue 41	-		✓		$C_{20}H_{26}N_4O_6S_2$	482.57
Reactive Red 120	-	✓			$C_{44}H_{24}Cl_2N_{14}Na_6O_{20}S_6$	1469.98
Disperse Red 324				✓	$C_{17}H_{17}Cl_2N_5O_4$	426.26
Basic Red 18	-		✓		$C_{19}H_{25}Cl_2N_5O_2$	426.34
Direct Red 80	-	✓			$C_{45}H_{26}N_{10}Na_6O_{21}S_6$	1373.08
Reactive Red 239		✓			$C_{31}H_{19}ClN_7Na_5O_{19}S_6$	1136.32
Reactive Red 84		✓			$C_{26}H_{19}BrN_4Na_2O_9S_3$	753.53
Disperse Green 9				✓	$C_{16}H_{18}N_6O_5S$	406.42
Reactive Red 158		✓			$C_{29}H_{22}ClN_7O_{11}S_3$	776.16
Reactive Blue 69		✓			$C_{23}H_{14}BrN_3Na_2O_9S_2$	666.39
Disperse Yellow 119				✓	$C_{15}H_{13}N_5O_4$	327.30
Food Dyes						
Acid Blue 9	Brilliant Blue FCF	✓			$C_{37}H_{42}N_4O_9S_3$	787.90
Acid Blue 74	Indigo Carmine	✓			$C_{16}H_8N_2Na_2O_8S_2$	466.35
Acid Yellow 3	Quinoline Yellow	✓			$C_{18}H_9N\ Na_2O_8S_2$	477.37
Acid Green 50	Green S	✓			$C_{27}H_{25}N_2NaO_7S_2$	576.62
Acid Red 14	Carmosine	✓			$C_{20}H_{12}N_2Na_2O_7S_2$	502.43

Appendix 2- Calibration

In order to understand the linear range it were determined the calibration lines for the used dyes.

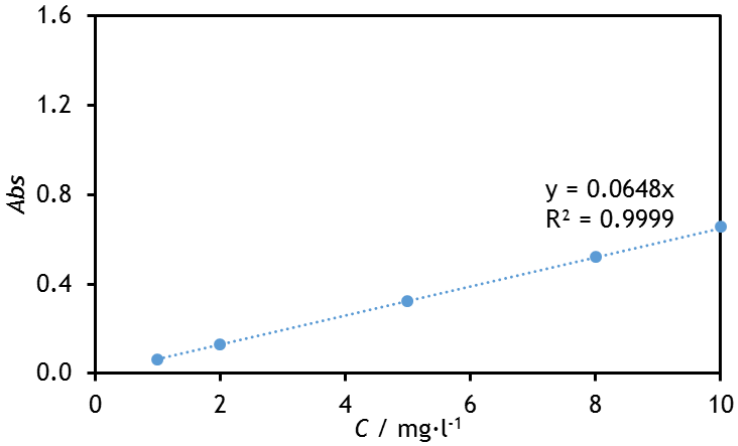

Figure 46 – Calibration line of the dye Chicago Sky Blue.

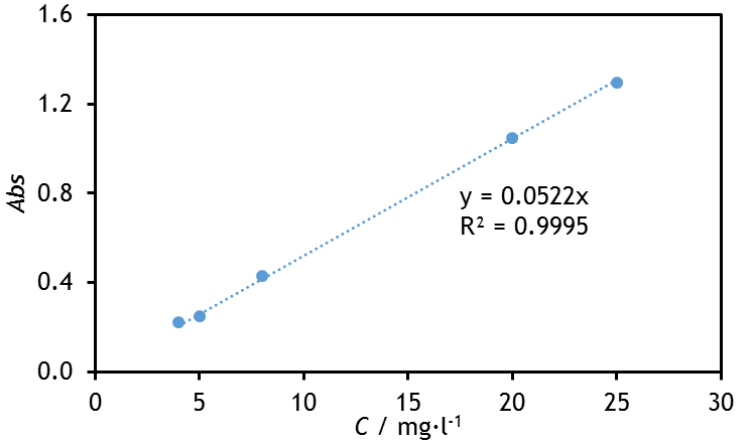

Figure 47 - Calibration line of the dye Orange II.

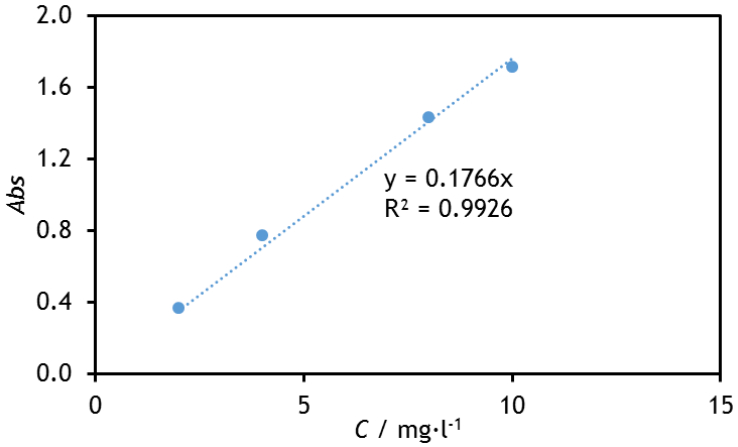

Figure 48 - Calibration line of the dye Methylene Blue.

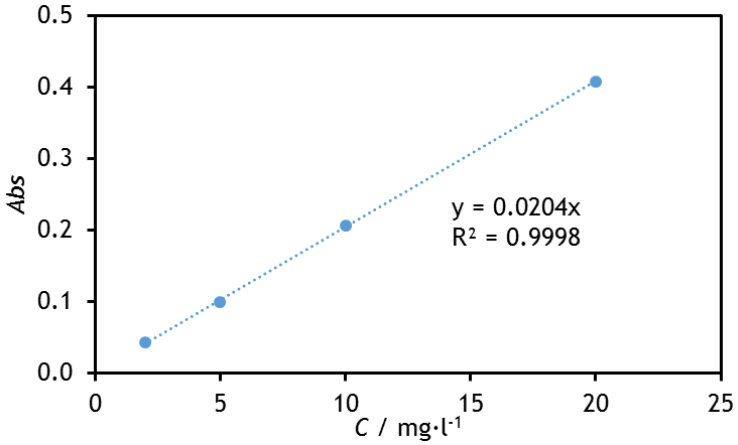

Figure 49 - Calibration line of the dye Basic Blue 41.

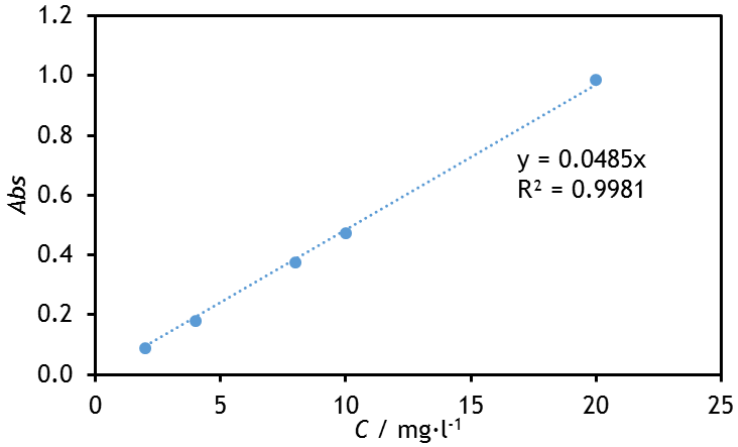

Figure 50 - Calibration line of the dye Basic Red 18.

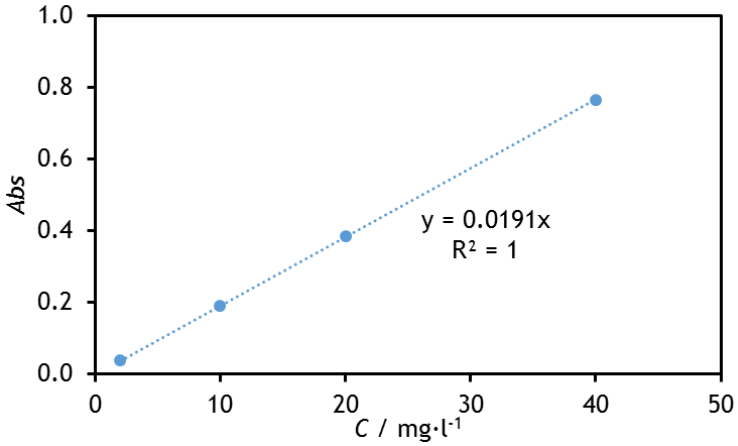

Figure 51 - Calibration line of the dye Reactive Red 239.

Appendix 3 - Adsorption Kinetics

In Figure 52 and Figure 53 are presented kinetic essays in order to compare the performance of two different adsorbents, MCM-41 and SBA-15. As it can be observed by the graphs, the adsorption of the MB dye is faster in the adsorbent MCM-41.

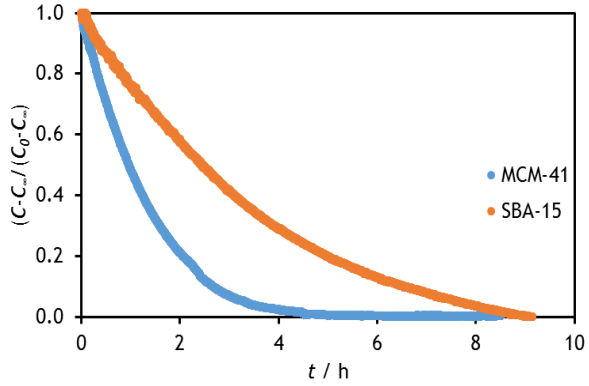

Figure 52 - Normalized concentration vs time for the adsorbents MCM-41 and SBA-15 with the dye MB.

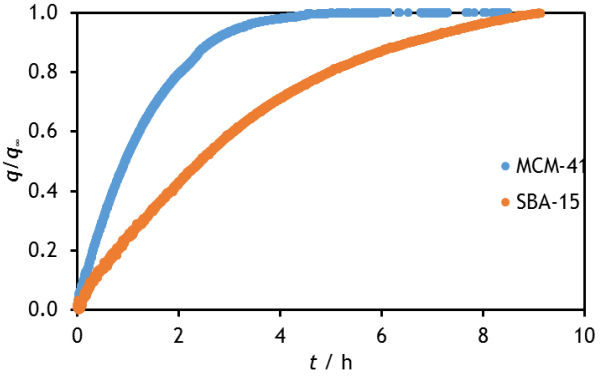

Figure 53 -Normalized adsorbed amount vs time for the adsorbents MCM-41 and SBA-15 with the dye MB.

In Figure 54 and Figure 55 are presented the essays which allows the comparison between the adsorbents MCM-41 and a carbon based xerogel. As it happened in the results above, the adsorption of the dye BB41 is faster on the adsorbent MCM-41 than on the other one.

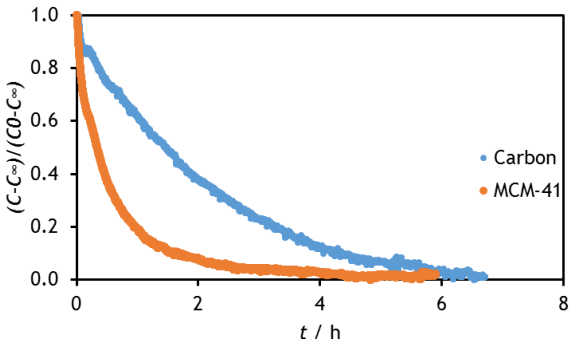

Figure 54 - Normalized concentration vs time for the adsorbents MCM-41 and activated carbon xerogel.

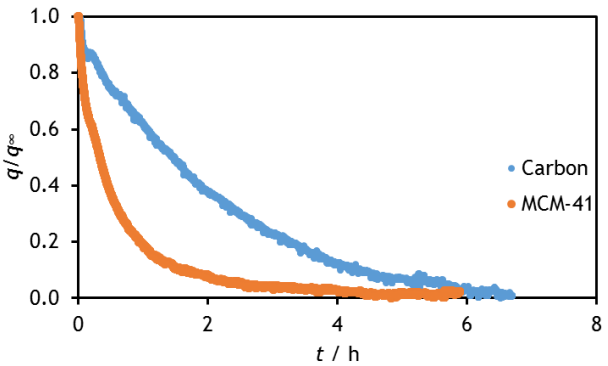

Figure 55 - Normalized adsorbed amount vs time for the adsorbents MCM-41 and activated carbon xerogel.

In Figure 56 and Figure 57 are presented the light absorption behavior of the mixture of the two dyes, MB and O II. It is shown in the graphs that the absorbance of the mixture does not stay constant during the time. This may be caused by the formation of a complex.

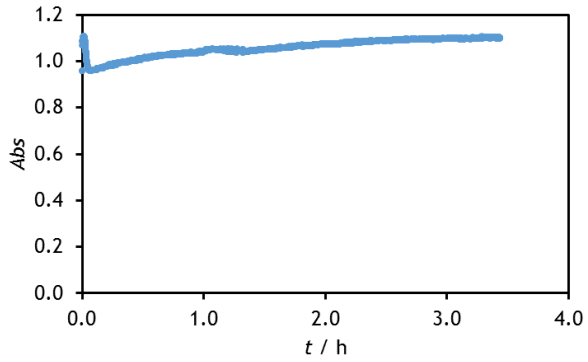

Figure 56 – Absorbance vs time for the dyes mixture MB and O II at a wavelength of 483 nm.

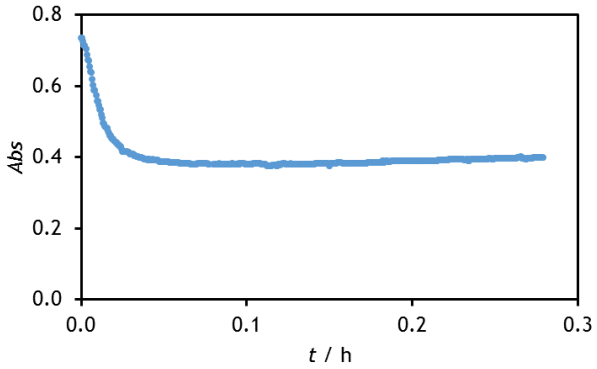

Figure 57 – Absorbance vs time for the dyes mixture MB and O II at a wavelength of 664 nm.

In Figure 58 and Figure 59 are presented the adsorption kinetics of the mixture of the dyes mentioned above with the adsorbent MCM-41. Once the dye O II does not adsorb on that adsorbent and the absorbance of MB is not so significant in the maximum wavelength of the dye O II, it is expected that the absorbance does not change a lot during the essay. On the other hand, the graph on the right side shows the variation of the absorbance on the maximum wavelength of MB, being expected each decrease, due to its adsorption onto the adsorbent.

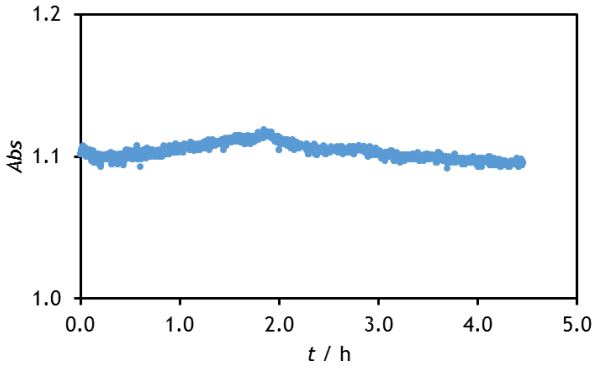

Figure 58 – Absorbance vs time for the mixture of dyes MB and O II with the adsorbent MCM-41 at a wavelength of 483 nm.

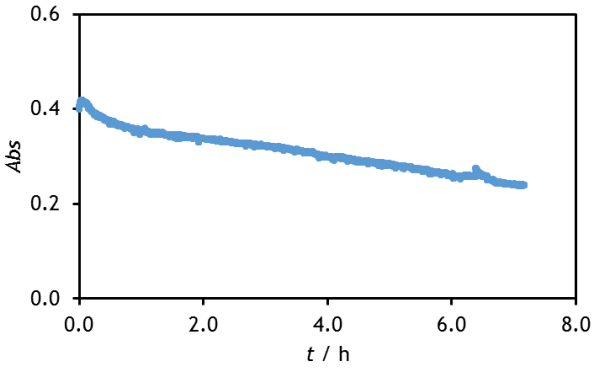

Figure 59 - Absorbance vs time for the mixture of dyes MB and O II with the adsorbent MCM-41 at a wavelength of 664 nm.

In Figure 60 are represented the essays performed in order to evaluate the kinetics of the mixture of two cationic dyes, BB41 and BR18.

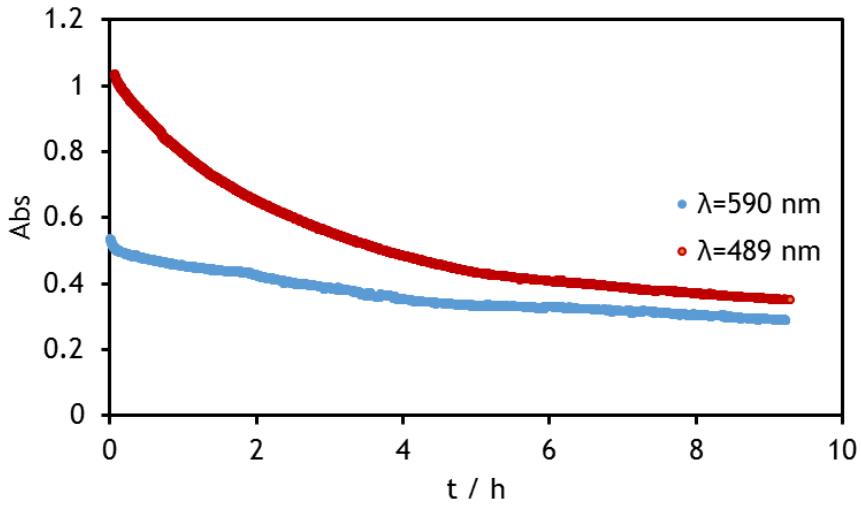

Figure 60 – Absorbance vs time for the mixture of BB41 and BR18 with the adsorbent MCM-41.

Appendix 4- Pulse Experiments

As it was already said, the pulse experiments were performed in metal column with metal tubes due to the cationic dye adsorption in the tubes, glass wool and glass spheres. In Figure 61 and Figure 62 are presented the tests in the first column, which has glass wool and glass spheres. From the second graphic, it is possible to understand that when the column is full with the spheres, (there is no adsorbent) the dye BB41 is retained in the column, being the curve correspondent to the column filled with spheres very similar to the curve of the column filled with the adsorbent. When the essay is only performed in the tubes without a column, it is possible to visualize the dye BB41, leaving the column, since the beginning of the experiment, discounting the space time.

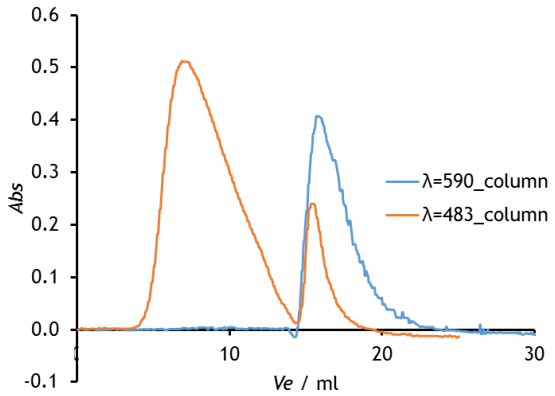

Figure 61 – Pulse response curves in the column experiment in both wavelengths.

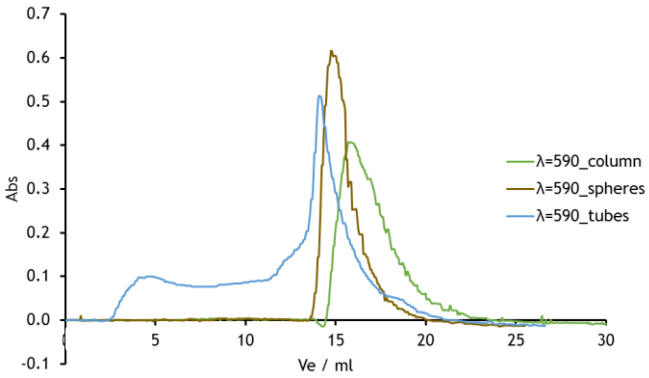

Figure 62 - Pulse response curves in the column, column filled with spheres and tubes at 590 nm wavelength.

Then it was noticed that the glass wool also adsorbs the dye BB41 and it was taken out of the column. The result is similar to the one obtained above once the dye sill adsorbs in the spheres. Therefore, the column was changed to a smaller one, which does not contain glass spheres on the inside, just the adsorbent. In this case, to perform the blank tests, metal spheres were used. The results obtained are represented in Figure 63 and Figure 64.

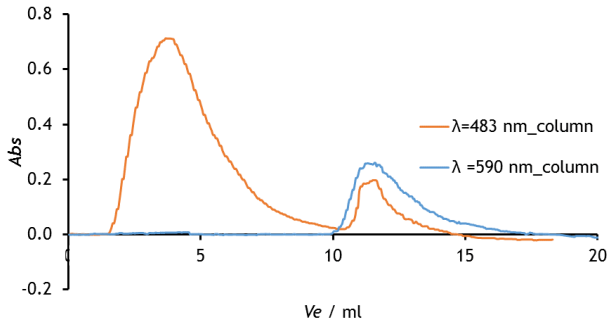

Figure 63 – Pulse response curves in the column without spheres.

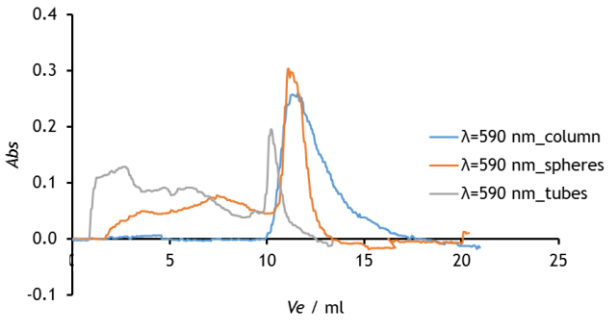

Figure 64 – Pulse response curves in the column, column filled with metal spheres and tubes.

The loop tube was made from silicone, so it also adsorbs the dye, being necessary to rotate back the loop valve after it is empty of the dyed solution. This can be proved from the Figure 65 once the curve correspondent to the column with the spheres without rotate back the loop valve, the blue one, has a larger peak in the maximum wavelength of the dye BB41 when the regeneration solution passes through the column, which means that a higher quantity of the dye leaves the column. The peak when the loop valve is not rotate back has a delay due to the increase of the space time.

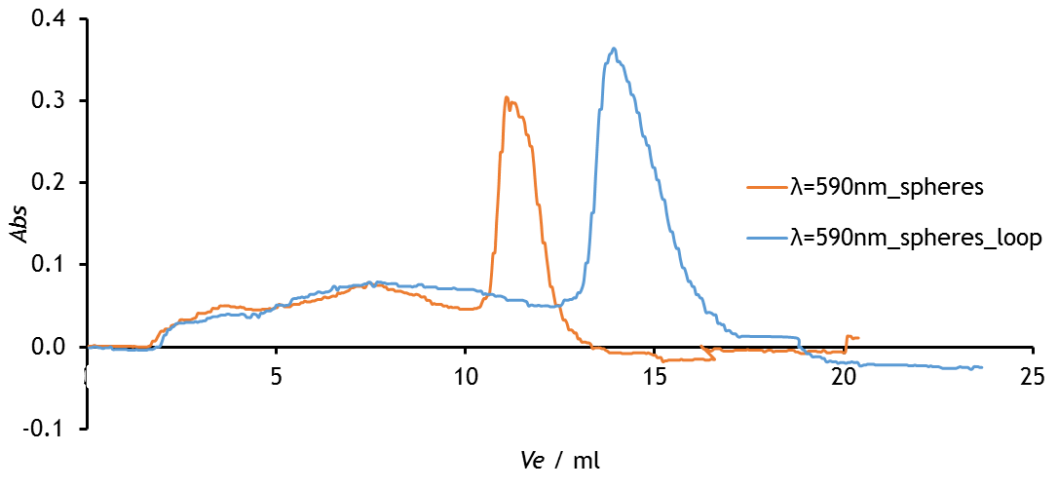

Figure 65 – Pulse curves for the column filled with spheres with and without rotating the loop valve.

Tests using dyes with the same charge were also performed. The dyes BB41 and BR18 were used with a concentration of 20 $mg \cdot l^{-1}$. Once both of them are cationic dyes, dye are adsorbed and they leave the column only with the regeneration solution, at the same time. The pulse response curves obtained are presented in Figure 66.

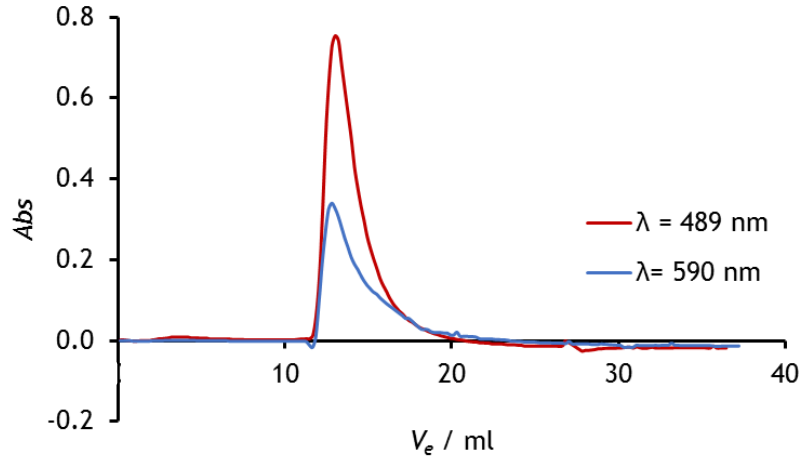

Figure 66 – Pulse curves in the column with the mixture of dyes BB41 and BR18.